Title
ATOMIC-DENSITY MEASUREMENTS IN A DECAYING HIGHLY IONIZED HYDROGEN PLASMA

Author
Forman, Peter Russell.

Publication Date
1966-10-31

UCRL-17177

University of California

Ernest O. Lawrence Radiation Laboratory

ATOMIC-DENSITY MEASUREMENTS IN
A DECAYING HIGHLY IONIZED HYDROGEN PLASMA

Berkeley, California

DISCLAIMER

Special thesis

UCRL-17177

UNIVERSITY OF CALIFORNIA
Lawrence Radiation Laboratory
Berkeley, California

AEC Contract No. W-7405-eng-48

ATOMIC-DENSITY MEASUREMENTS IN A DECAYING HIGHLY IONIZED HYDROGEN PLASMA

Peter Russell Forman
(Ph. D. Thesis)

October 31, 1966

ATOMIC-DENSITY MEASUREMENTS IN A DECAYING HIGHLY IONIZED HYDROGEN PLASMA

Contents

ATOMIC-DENSITY MEASUREMENTS IN A DECAYING HIGHLY IONIZED HYDROGEN PLASMA

Peter Russell Forman

Lawrence Radiation Laboratory
University of California
Berkeley, California

October 31, 1966

ABSTRACT

Atomic-density measurements in a decaying, dense, highly ionized hydrogen plasma have been performed by a vacuum uv-absorption technique. Light of wavelength 890.8 Å is shone through the plasma, and its attenuation, caused by photoionization of the hydrogen atoms present, is measured. The plasma is formed in a copper cylinder 86.4 cm long with a radius of 7.3 cm. In the interior, the initially highly ionized plasma, which has an ion density of 4.9×10^{15} ions/cc and a temperature of about 1 eV, is found to decay by three-body volume recombination. Its atomic density is observed to increase in time at the correct rate, which confirms the earlier notion that this part of the plasma indeed recombines in situ, and remains near Saha equilibrium for up to 200 μsec. During the formation of the plasma apparently a layer of atoms is formed near the cylinder wall. This layer has been detected and observed to relax in a time consistent with diffusion inward due to charge-exchange collisions with the ions of the plasma. The energy loss in the interior regions of this plasma is observed to be at a rate considerably in excess of that expected from normal thermal conductivity or even from anomalous diffusion of ions.

I. INTRODUCTION

This thesis reports the experimental investigation of the decay of a dense, highly ionized, hydrogen plasma by spectroscopic determination of the atomic density and the electron density and temperature as functions of position and time.

The disappearance of hydrogen plasmas has been observed for a number of years. One of the first observations was made by Lord Rayleigh in 1944 when he noticed the persistence of light in an electrodeless discharge after the current had been turned off.[1] He correctly suggested that this light arises from electrons recombining with ions. Since then there have been numerous experiments characterized by increasing accuracy of measurement and better theoretical interpretations.[2-6] Craggs and Meek[7] observed the recombination light in a spark discharge and compared their results with the theoretical rate obtained by Zanstra.[8] The latter rate, which was based on the assumption that the dominant loss mechanism was radiative recombination, turned out to be an order of magnitude too small. D'Angelo showed that this discrepancy could be removed if one were to assume that a second process, three-body recombination (the inverse of collisional ionization), was also present.[9] With the aid of high-speed computers it has become possible to calculate the recombination-rate coefficient limited in accuracy to the uncertainty in the cross sections employed in the calculations. Several such calculations have been performed.[10-12] That of Bates, Kingston, and McWhirter is discussed briefly in the next section.[13,14]

All of the experiments have been performed by measuring the ion (electron) density as a function of time and comparing these measurements with the equation

$$\frac{DN_i}{Dt} = - \gamma(N_e T) N_i N_e . \qquad (1)$$

It should be noted that if volume recombination is the process that is determining the time rate of change of the ion density, then the change

of the atomic density with time must just equal minus the change in the ion density. To exclude the possibility that other processes are occurring it would seem necessary to determine that the atomic density is indeed building up at the same rate that the ion density is decreasing.

In an experiment performed previously at this laboratory a number of questions were left unanswered, all of which were related to the total lack of information as to the atomic density. These were: (1) The initial degree of ionization was unknown. (2) Many measurements of the plasma indicated that the initial degree of ionization should be very high, yet the observed ion density was some 20% below the initial filling. The question remained as to where these atoms had gone if the plasma were indeed highly ionized. (3) A knowledge of the atomic density and its gradient was necessary to estimate the contribution of diffusion by charge exchange to the observed rate of change of the ion density. (4) The electron temperature near the edge of the plasma as measured by several spectroscopic techniques showed serious disagreement (see Appendix B).

These lingering questions about the existing plasma, combined with the fact that it seems no one has measured the atomic density in a highly ionized recombining hydrogen plasma, prompted this experiment.

II. THEORY

A. Recombination-Rate Coefficient

Bates, Kingston, and McWhirter have performed numerical calculations of the decay coefficient of hydrogen and helium plasmas considering radiative and collisional interactions.[13,14] The salient features of their calculations are outlined here. Only the cases of interest for comparison with the experiment are included. The processes included in their work are as follows.

1. Collisional ionization and its inverse, three-body recombination:

$$H(n) + e \rightleftarrows H^+ + e + e. \tag{2}$$

2. Collisionally induced transitions between discrete levels;

$$H(n) + e \rightleftarrows H(m) + e. \tag{3}$$

3. Radiative recombination:

$$H^+ + e \rightarrow H(n) + h\nu. \tag{4}$$

4. Spontaneous emission:

$$H(n) \rightarrow H(m) + h\nu. \tag{5}$$

The rate of change of the populations of the various discrete levels of the hydrogen atom then form an infinite set of coupled linear equations of the form

$$\frac{\partial N(n)}{\partial t} = F_n\left[N(j),\ T,\ N_e,\ X\right], \tag{6}$$

where j is a running index that extends over all of the principal quantum numbers, T is the electron temperature, N_e is the electron density, and X represents appropriate atomic parameters.

Two limiting cases of interest for comparison with this experiment were considered. In one the plasma is considered to be optically thin,

i.e., all radiation escapes; in the other the plasma is optically thick for the Lyman series but thin for all others. To render the computation tractable, we assume that the number of atoms in any excited state is very much less than the electron density,

$$N(n) \ll N_e, \qquad n \neq 1, \tag{7}$$

and further

$$N(n) \ll N(1), \quad n \neq 1. \tag{8}$$

This has the effect that "the relaxation times for the excited levels are very much shorter than the relaxation time for the ground level or for the free electrons".

These assumptions imply that the excited states are in quasi-steady state, allowing their time derivatives to be set equal to zero. This alters the infinite set of equations to the form

$$\frac{\partial N(1)}{\partial t} = F_1\left[N(j),\ T,\ N_e,\ \chi\right] \tag{9}$$

$$0 \quad = F_n\left[N(j),\ T,\ N_e,\ \chi\right] \quad n \neq 1.$$

States with principal quantum number above some value "s" (to be defined) are assumed to be in Saha equilibrium with the free electrons. This reduces the infinite set of equations to a finite set.

To define s the equation

$$N(n) \equiv \rho(n) N_{eq}(n) \tag{10}$$

is introduced, where N(n) is the calculated value of the number density of atoms in the nth state, and $N_{eq}(n)$ is the equilibrium value for N(n) for the same assumed electron temperature and density.

The reason that the upper quantum states can never be in exact equilibrium in this calculation is that there is no process corresponding to photo absorption. Spontaneous emission therefore represents a sink for which there is no corresponding source, as required for detailed balance. If the transition probabilities are proportional

to n^{-3} and the collisional cross sections are roughly proportional to n^4, it can be seen that for the higher quantuum levels the collisional processes will dominate the population and depopulation of these levels. One would then expect $\rho(n)$ to be a very strong function of n. This fact was employed in the definition of s. The definition is $\rho(n)_{n=s-1} \equiv 0.5$. With this definition it is expected that $\rho(s+1)$ will indeed by very close to unity. The procedure then was to assume a value for s and calculate $\rho(s-1)$. If it was too small the calculation was redone with a larger s.

The equations left to be solved are (changing their notation somewhat):

$$\frac{\partial N_n}{\partial t}\,\delta_{in} = -N_n N_e K(n) \qquad \text{collisional ionization and collisionally induced transitions to other bound states}$$

$$= -N_n A_n(m<n) \qquad \text{spontaneous transitions to lower states}$$

$$= +N_e \sum_{m\neq n} N_m K(m,n) \qquad \text{population by collisionally induced transitions from other bound states}$$

$$= +\sum_{m>n} N_m A(m,n) \qquad \text{population by radiative transitions from higher bound states}$$

$$= +N_i N_e K(N_e,n) \qquad \text{three-body recombination}$$

$$= +N_i N_e \beta(n) \qquad \text{radiative recombinations to nth state,} \qquad (11)$$

where δ_{in} is the Kronecker δ, and K, A, and β are the appropriate rate coefficients.

To evaluate the rate coefficients of Eq.(11), cross sections and transition probabilities from various sources were used. For the spontaneous transition probabilities, the tables of Baker and Menzel[15] and of Green, Rush, and Chandler were used.[16] The radiative recombination coefficients were obtained from the tables of Seaton.[12]

The rate coefficients for the collisional excitations and collisional ionizations were evaluated using the classical cross sections derived by Gryzinski[17] and assuming that the electrons have a Maxwellian distribution.

The quantity that Bates et al. obtain is $\gamma(N_e, T)$

$$\frac{\partial N_1}{\partial t} = + \gamma(N_e, T) N_e N_1. \tag{12}$$

Under the conditions that they assume their γ is the same as the γ of Eq. (1). This is true because the electrons that disappear from the continuum reappear in the ground state. They express their calculated recombination decay coefficient in two parts, $\gamma = \alpha - S(N_1/N_e)$, where α is called the collisional-radiative recombination coefficient and S is the collisional-radiative ionization coefficient. A plot of α and S as a function of temperature for various electron densities is shown in Figs. 1 and 2.

In a second paper the same authors consider the case where the plasma is considered to be optically thick for the lines of the Lyman series.[14] This was accomplished by simply leaving out the terms that in the original rate equations correspond to population and depopulation of the ground state by radiative processes with the exception of radiative recombination. In defining their results they found it necessary to consider the second state (n = 2) not to be in quasi equilibrium. They express their results in terms of the densities in n = 1 and n = 2 states. Since the procedure was essentially the same as before, the details will not be discussed here. The resulting values of α are also included in Fig. 1, however.

B. Vacuum-Ultraviolet Absorption Theory

Since the first excited state of hydrogen is 10.2 eV above the ground state, in a plasma with a temperature of 1 to 2 eV (if anything remotely near equilibrium exists) the preponderance of atoms present must be in the ground state. By definition the ground state

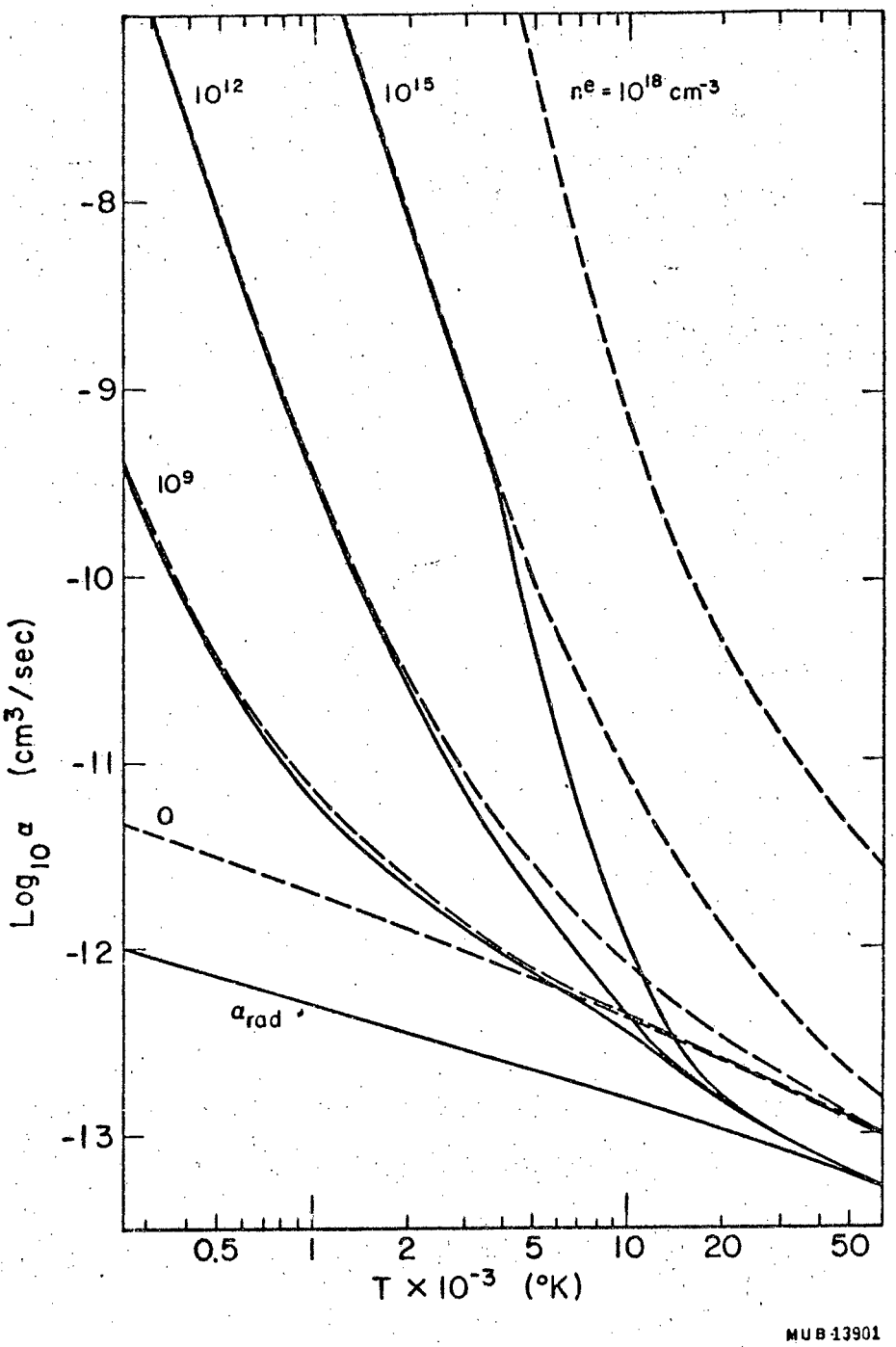

Fig. 1. Collisional-radiative recombination coefficient for electrons and atomic hydrogen ions as a function of electron temperature at several electron densities. Solid curves: plasma transparent except to Lyman line radiation. Dashed curves: plasma transparent to all radication.

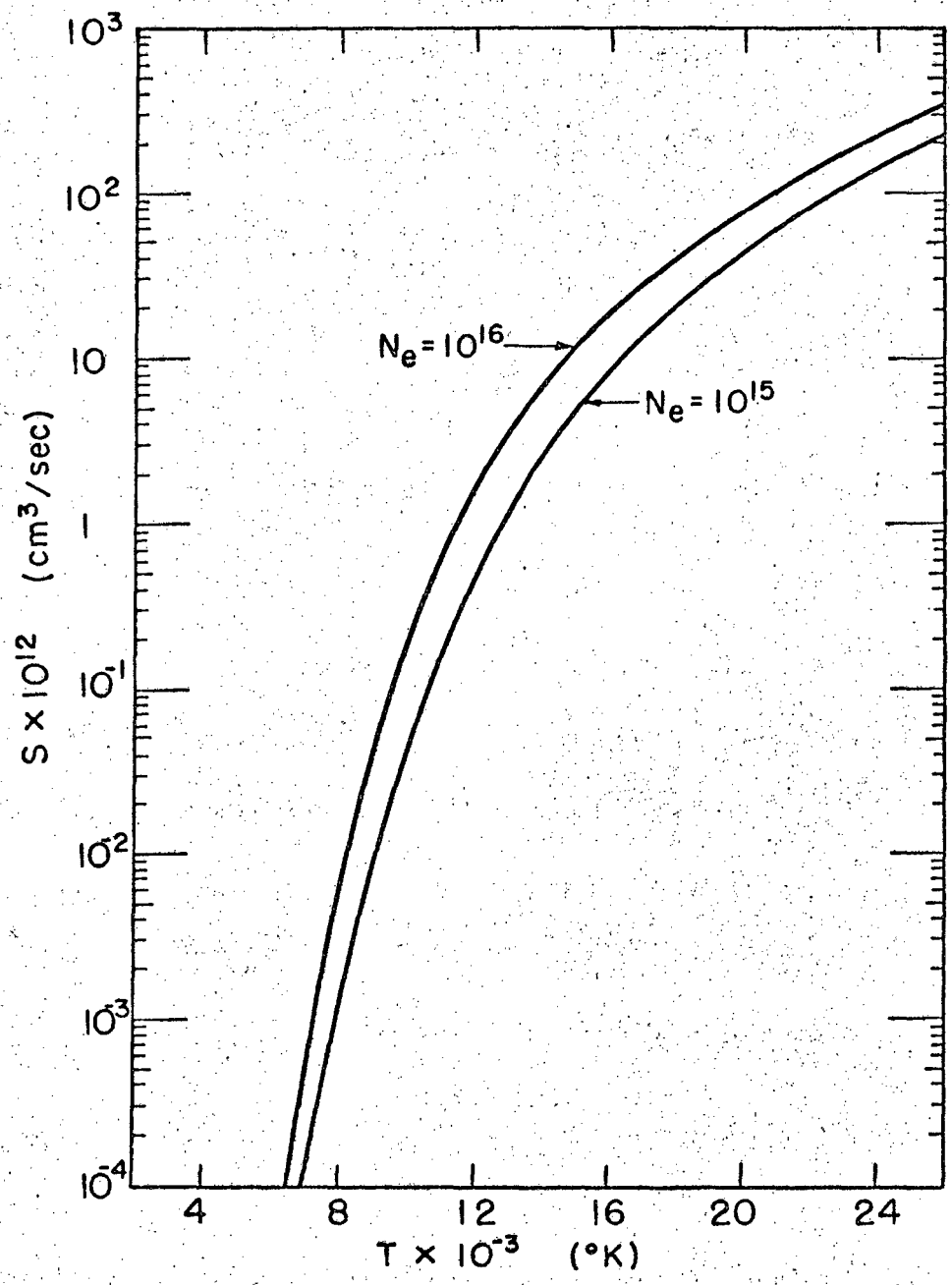

Fig. 2. Collisional-radiative ionization coefficient as a function of temperature for two electron densities.

does not radiate; therefore if a spectroscopic measurement is employed, it must be done by absorption.

Two types of transmission experiments immediately come to mind. The first would use light corresponding to one of the Lyman lines, for example L_α (1215.7 Å, $n = 1 \rightarrow n = 2$). This would have the advantage that the absorption cross section is very large, and hence would be a very sensitive measure of the ground-state atomic density. There are, however, sufficient complications to make such an experiment unattractive. While the absorption cross section is large, its exact frequency dependence is not known, because it depends on the plasma conditions (density and temperature) since both Doppler broadening and Stark broadening will be present. Line absorption of line radiation would then seem impractical. This objection could be removed if the incident light was a band of continuum with a width greater than the possible absorption line width. If this criterion is met, no knowledge of the broadening mechanisms is necessary. This brings up the second obstacle.

Unfortunately, it is not at all clear exactly what to use for such a continuum light source. Its requirements are rather severe, as it must be borne in mind that the plasma under investigation is itself often an extremely strong radiator of Lyman lines. The continuum light source would have to be either (1) brighter than the plasma, or (2) repetitive so that phase-locking technqiues could be employed. Because the plasma to be investigated lasted approximately 200 μsec repeated at most every 45 sec, phase-locking techniques seemed useless. In addition, the prospect of obtaining a source brighter than the plasma seemed equally hopeless. This mode of experimentaion was discarded as impractical.

The second spectroscopic method available is to induce transitions from the ground state to the continuum rather than to some excited state. One is then interested in the photoionization cross section for wavelengths less than 912 Å. Because the photoionization cross section is a smooth, slowly varying function of frequency, and

hence is insensitive to any line broadening, it was decided to employ this technique. Further, line radiation could be used for the light source, and the prospect of obtaining a source brighter than the plasma is greatly increased.

To interpret the results of such a transmission measurement, one must have a knowledge of the total absorption cross section, including all possible processes. In a laboratory hydrogen plasma, one should expect to find protons, electrons, neutral hydrogen atoms, negative hydrogen ions, hydrogen molecules, impurity ions, atoms and molecules. The effect of each of these will be discussed.

The first to be considered is the desired term, that of the atomic hydrogen. The photoionization cross section for atomic hydrogen can be calculated exactly and can be expressed as[18]

$$\sigma_{(\nu,n)} = \bar{g}\left[\frac{64\pi^2 e^{10} m_e}{3\sqrt{3}\, ch^6}\right]\frac{1}{\nu^3 n^5} . \tag{13}$$

Here n is the principal quantum number, $\bar{g}$ is a Gaunt factor averaged over angular-momentum states to correct the classical expression to agree with quantum mechanics. These Gaunt factors are of order one.

For convenience, we can express the absorption due to all excited states in terms of the ground-state density and a temperature, assuming a Boltzmann distribution of excited states. Because of the strong dependence of the cross section upon principal quantum number, this is expected to introduce little error if the ground state is not too far from equilibrium with the excited states.

One may express this absorption coefficient by

$$K_H(\nu,T) = \frac{64\pi^4 m_e e^{10}}{3\sqrt{3}\, ch^3 (kT)^3}\,\frac{e^{-u_1}}{u^3}\left\{\sum_{u_n < u}^{u_{n(max)}} (\bar{g}_{fb})_n \frac{e^{u_n}}{n^3} + \frac{1}{2u_1}\,\bar{g}_{fb}\left[\exp\left(u_{n(max+1)} - 1\right]\right\}, \tag{14}$$

where m_e and e are the mass and charge of the electron, $u = h\nu/kT$, and $u_n = \chi_n/kT$. k is Boltzmann's constant, h is Planck's constant, and c is velocity of light. Here χ_n is the energy of the nth quantum state and n the principal quantuum number.

The upper limit of the summation needs further explanation. In a plasma there is a lowering of the ionization potential because of the electric fields of neighboring ions and electrons. As a result the number of bound states of the hydrogen atom in a plasma is reduced. Griem[19] has shown that it is consistent to assume that the last bound state (having principal quantum number n_{max}) satisfies the equation

$$\chi_{n(max)} = \frac{e^2}{\left[kT/4\pi e^2 N_e\right]^{1/2}} . \qquad (15)$$

This was the definition of n_{max} used in the computer calculations.

Absorption of light due to hydrogen molecules fortunately can be avoided. The absorption cross section of molecular hydrogen has been measured.[20] It does not become appreciable until below about 860 Å. To absorb appreciably the photon must have sufficient energy to excite the $^1\pi_u(3p)$ state of the molecule. This sets a lower limit on the allowed wavelength in the search for a suitable light source.

The H^- absorption can also be expressed per atom in the ground state, since the ionization potential of the H^- ion is only 0.74296 eV. For reasonable electron temperatures the number of H^- ions can be related to the actual ground-state atom density by Saha's equation:

$$S_{H^-}(T) = \frac{N_1 N_e}{N_{H^-}} = \frac{g_e g_1}{g_{H^-}} \frac{(2\pi m_e kT)^{3/2}}{h^3} \exp\left[-(\chi_{H^-}/kT)\right], \qquad (16)$$

with $g_e = g_1 = 2$, $g_{H^-} = 1$, and $\chi_{H^-} = 0.7496$ eV.

We define K_{H^-} as the absorption coefficient due to H^- ions per atom in the ground state:

$$K_{H^-}(\nu, T_e, N_e) = \frac{N_e h^3 e^{0.7496/kT}}{4(2\pi m_e kT)^{3/2}} \xi(\nu). \qquad (17)$$

The tables of Ref. 21 were used to estimate the ratio K_{H^-}/K_H for $2500^\circ K < T_e < 20\,000^\circ K$ and $n_e < 10^{16}$, and this ratio is always less than 10^{-2}. Absorption by H^- ions can be ignored.

Next we consider the effect of impurities in the plasma. Figure 3 is a spectrum of the plasma investigated in this thesis. It was taken with a small Hilger quartz-prism spectrograph. The scale in Fig. 3 is in 10^{-2} Å. The broadened lines are the Balmer hydrogen series followed by its continuum. Also apparent are a number of faint sharp lines. These have been identified as coming from Cu I, Al I, C II, Si II, Si III, Si IV, O I, and O II. The absorption cross sections for these elements are expected to be smaller or comparable to that of hydrogen in the region of interest;[22,23] however, their number density will be vastly smaller.[24] The only way that impurities could influence the measurement then is by an accidental choice of frequency that happened to match some allowed transition in one of these atoms or ions. In this case the absorption cross section would become very large and the presence of such an impurity might well influence the measurement. In order to avoid this these elements are ruled out as possible candidates for the light source.

An electron or proton by itself can only affect the light by Compton scattering, which is totally negligible in comparison with atomic photoionization; however, collectively they can absorb light by free-free transitions (inverse bremsstrahlung). The absorption coefficient per atom in the ground state can readily be computed as were the free-bound transitions. Equation (14) now becomes

$$K_\nu = \frac{64\pi^4 m_e e^{10}}{3\sqrt{3}\, ch^3 (kT)^3} \frac{e^{-u_1}}{u^3} \left\{ \sum_{u_n < u}^{u_{n(max)}} (\bar{g}_{fb})_n \frac{e^{u_n}}{n^3} + \frac{1}{2u_1}\left[g_{fb}\left[\exp(u_{n(max+1)}) - 1\right] + \bar{g}_{ff}\right] \right\}, \qquad (18)$$

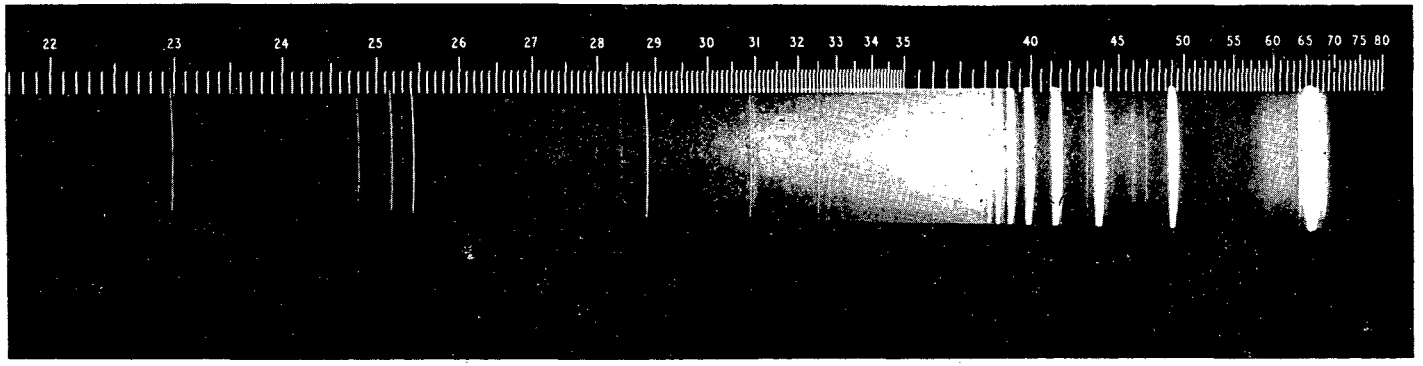

ZN-3832

Fig. 3. Spectrum of the hydrogen plasma.

where again the number of atoms in the ground state has been assumed to be in equilibrium with the electrons. Coefficient K_ν was calculated by computer as a function of electron density and temperature, with Gaunt factors taken from the tables of Karzas and Letter[25] for $\lambda = 890$ Å. In the region shown in Fig. 4 for electron densities up to 10^{16}, there is no density dependence.

The one unfortunate but essential assumption in the preceding is that the ground state is in equilibrium. If the number of ground-state atoms is higher than the number in equilibrium, that is fine. The trouble in this experiment would arise when the number fell below its equilibrium value. The effect of this assumption can be estimated by performing the following calculation.

One may express the absorption coefficient as

$$K_\nu \equiv \sigma + K_\nu', \tag{19}$$

where σ is the photoionization cross section for a ground-state hydrogen atom. Using the definition given in Eq. (10), i.e., $N(1) = \rho(1)\, N_{eq}(1)$, we can express the absorption coefficient as

$$K_\nu = \sigma + \frac{K_\nu'}{\rho(1)}, \tag{20}$$

The effect of varying $\rho(1)$ then is to keep all of the excited states in Saha equilibrium with the free electrons while varying the ground-state population. A plot of the absorption coefficient as a function of temperature for several $\rho(1)$'s is shown in Fig. 4. It can be seen that this approximation could have serious effects for temperatures above 15 000°K. For all times of interest the plasma studied has a temperature below 15 000°K. The hypothetical requirement of Fig. 4 [$\rho(1)$ is 0.01, while the rest of the bound states of the atom are at their equilibrium values] is far too severe. If it were necessary a more reasonable approach would be to employ the quasi-steady-state values of $\rho(n)$ calculated by Bates et al.[26] This would be valid if

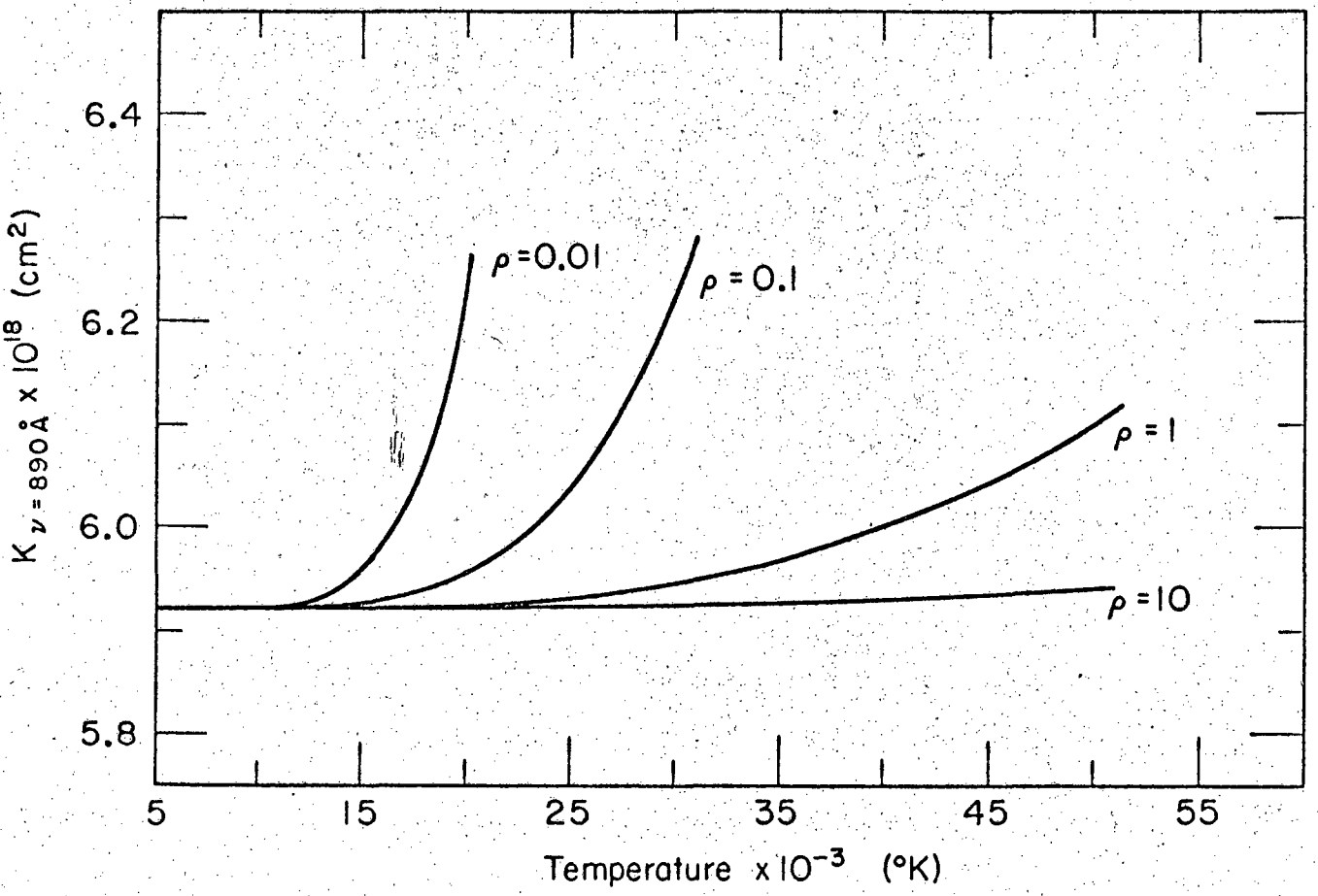

MUB-12995

Fig. 4. Absorption coefficient per hydrogen atom in the ground state as a function of temperature for several values of ρ(1).

the observed rates of change of the electron temperature and density were slow compared with the population and depopulation rates of the various levels.

Once one knows the absorption coefficient, measurement of the atomic density is straightforward. The intensity of a beam of light of frequency interval $d\nu$ passing through a plasma containing hydrogen atoms obeys Lambert's law

$$I(\nu)d\nu = I_0(\nu) \exp\left(- k_\nu \int_0^L N(x)dx\right)d\nu, \qquad (21)$$

where $N(x)$ is the atomic density distribution along the length of the plasma.

The signal received by a detector is an integral over some frequency interval. Because the photoionization cross section is a slowly varying function of frequency and the band pass of a monochromator is narrow, combined with the fact that in this region of the spectrum the light source used* emits primarily light of 890.84 Å, the light can be considered as monochromatic.

The atomic-density distribution along the length of the machine may be divided into (1) some distribution at the ends, and (2) the distribution throughout the length of the cylinder:

$$\int_0^{L_0} N_1(x)dx + \int_{L_0}^{L} N_2(x)dx = \frac{1}{K_\nu(\nu_0)} \ln \frac{I_0}{I} = \frac{1}{K_\nu(\nu_0)} \ln R, \qquad (22)$$

where L_0 represents some dividing point.

If then, two measurements are made with different cylinder lengths, and it is assumed that the plasma decays in the same fashion, in particular that the end effects develop in the same way, the difference of the two measurements yields

---

*Described in Section (IIIC).

$$\int_{L_1}^{L_2} N_2(x) = \frac{1}{K_\nu(\nu_0)} \ln \frac{R_2}{R_1} \tag{23}$$

or

$$(N_2) \equiv \frac{1}{K_\nu(\nu_0)\left[L_2 - L_1\right]} \ln \frac{R_2}{R_1} . \tag{23}$$

This means end effects can be subtracted out if absorption measurements are performed on plasmas that are identical except for their length.

C. Visible and Near-Ultraviolet Measurements for Electron Density and Temperature Determinations

Consider a hydrogen plasma in local thermodynamic equilibrium in the sense that there is a well-defined electron temperature. Continuum radiation coming from such a plasma arises primarily from (1) free-free transitions (bremsstrahlung) represented by the equation

$$H^+ + e \rightarrow H^+ + e + h\nu, \tag{25}$$

and (2) free-bound transitions (radiative recombination) represented by

$$H^+ + e \rightarrow H_n^* + h\nu, \tag{26}$$

where H_n is the nth quantum state of the hydrogen atom. The power radiated per (cm^3, steradian, second, Angstrom) from such reactions can be expressed in the form

$$I_c(N_e \nu T_e) = N_i N_e W_e(\nu, T_e). \tag{27}$$

Line radiation also is emitted from such a plasma, the intensity of which is

$$I_\ell = N_n A_{nm} h\nu_{nm}, \tag{28}$$

where N_n is the number of atoms in the quantum state n, A_{nm} is the

transition probability from state n to m, ν_{nm} is the frequency of such radiation, and h is Planck's constant. If the upper state is in equilibrium with the free electrons, it can be related to the free-electron density through Saha's equation

$$\frac{N_i N_e}{N_n} = S(T_e, \chi_n), \tag{29}$$

where χ_n is the ionization potential of the atom in the nth state. Hence the intensity of the light emitted in any of the hydrogen lines, where the upper state meets the equilibrium condition, may also be expressed in the form

$$I_\ell = N_i N_e W_\ell(\nu_\ell, T_e). \tag{30}$$

We see therefore that both the ratio of the energy emitted in a particular line to that in a band of continuum and the ratio of two bands of continuum are a function of electron temperature and not of the electron density. In addition, once the electron temperature is known, an absolute measure of the emitted light is a measure of the electron density if $N_i = N_e$. In practice, in a plasma the ionization potential is lowered due to the collective effect of the electric fields of the neighboring ions and electrons. This reduction of the ionization potential results in a small variance from the $N_i N_e$ dependence of the continuum radiation, which can be seen in Figs. 6 and 7. Figures 5 through 10 were obtained by a computer calculation of Eq. (18) using Kirchoff's law to relate the absorption coefficient to the emission coefficient (see Appendix A).

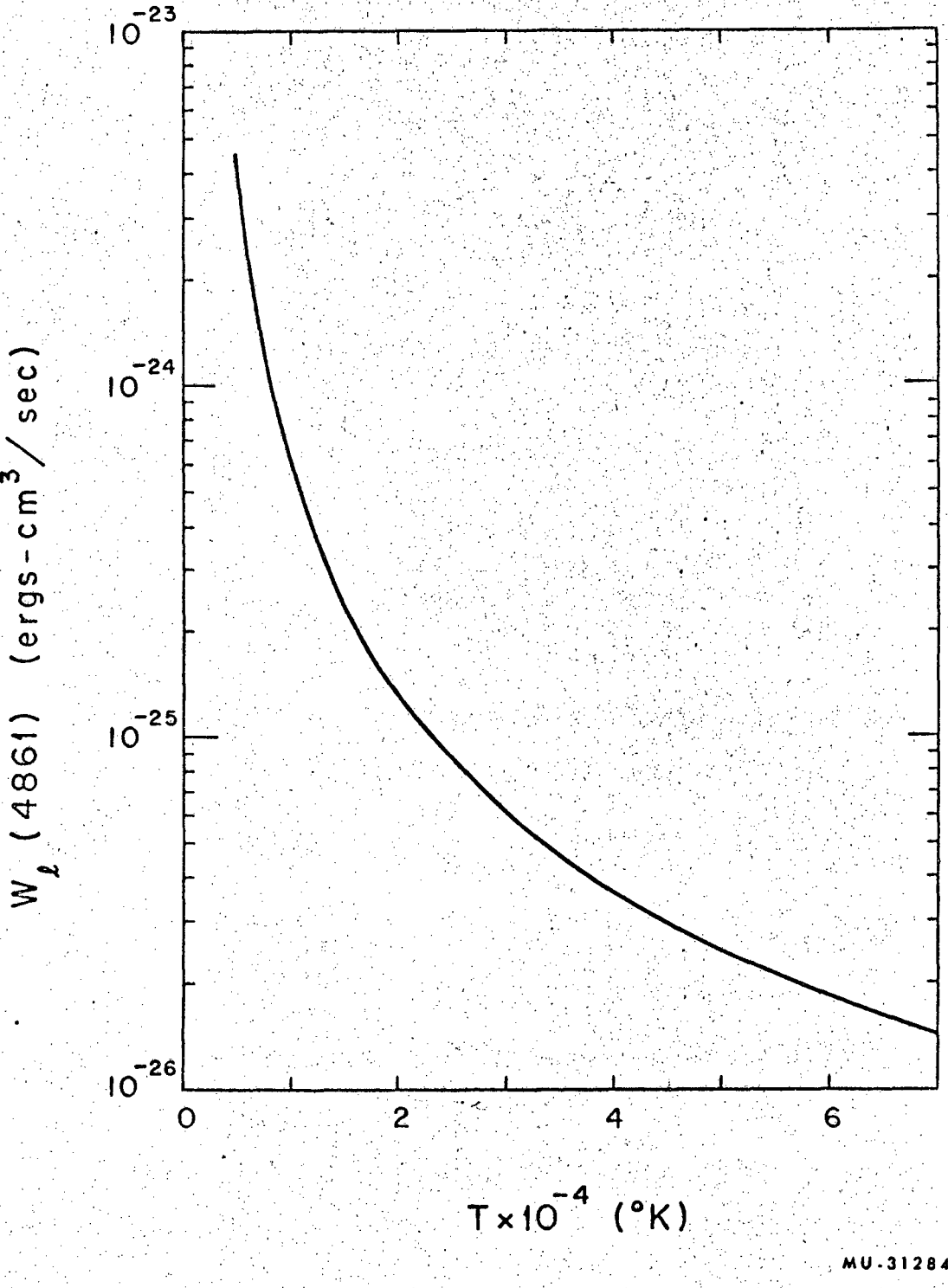

Fig. 5. Normalized H_β-line intensity $W_\ell(4861)$ as a function of temperature.

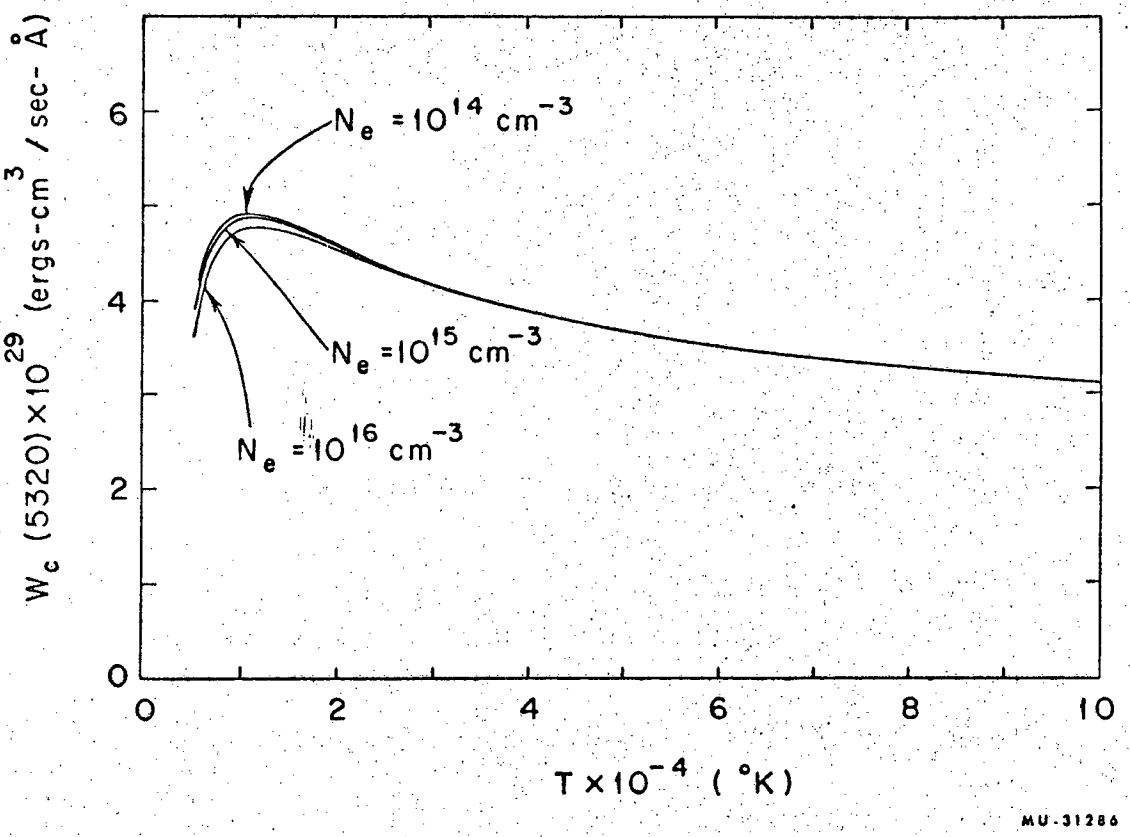

Fig. 6. Normalized continuum intensity $W_c(5320)$ at λ = 5320 Å as a function of temperature.

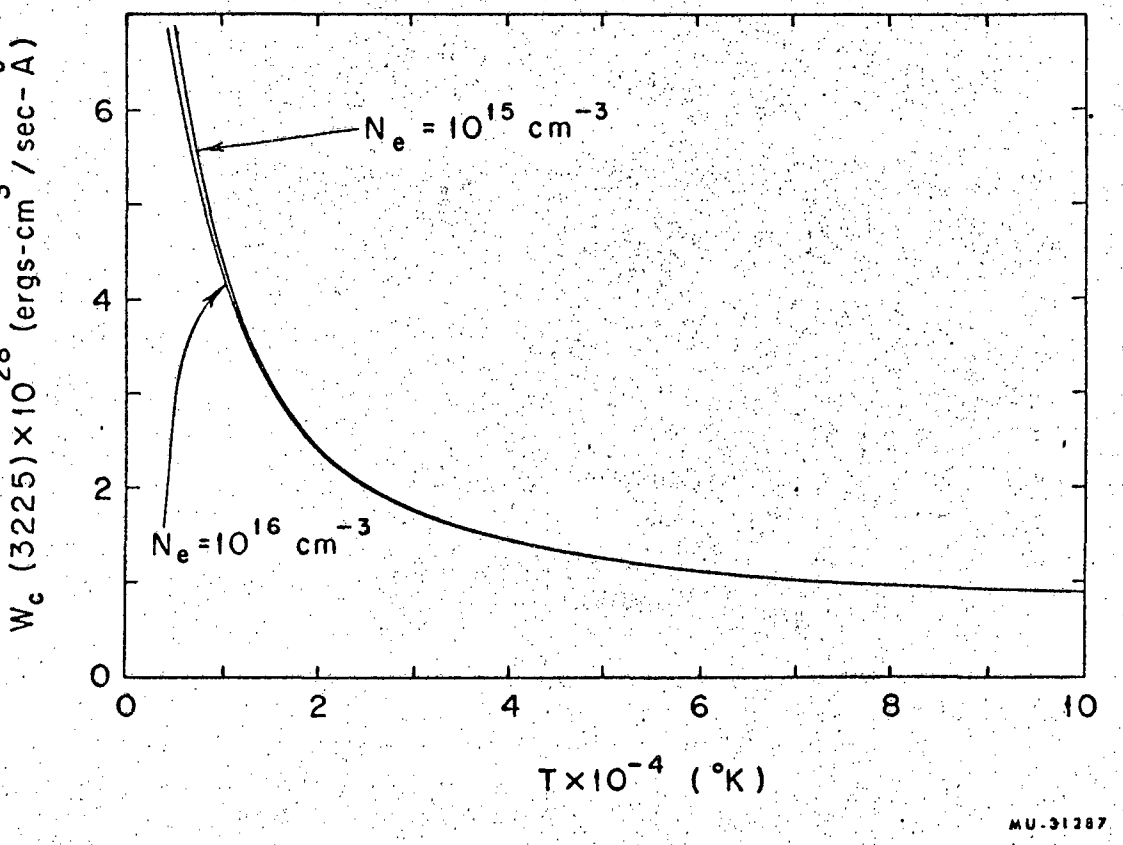

Fig. 7. Normalized continuum intensity $W_c(3225)$ at $\lambda = 3225$ Å as a function of temperature.

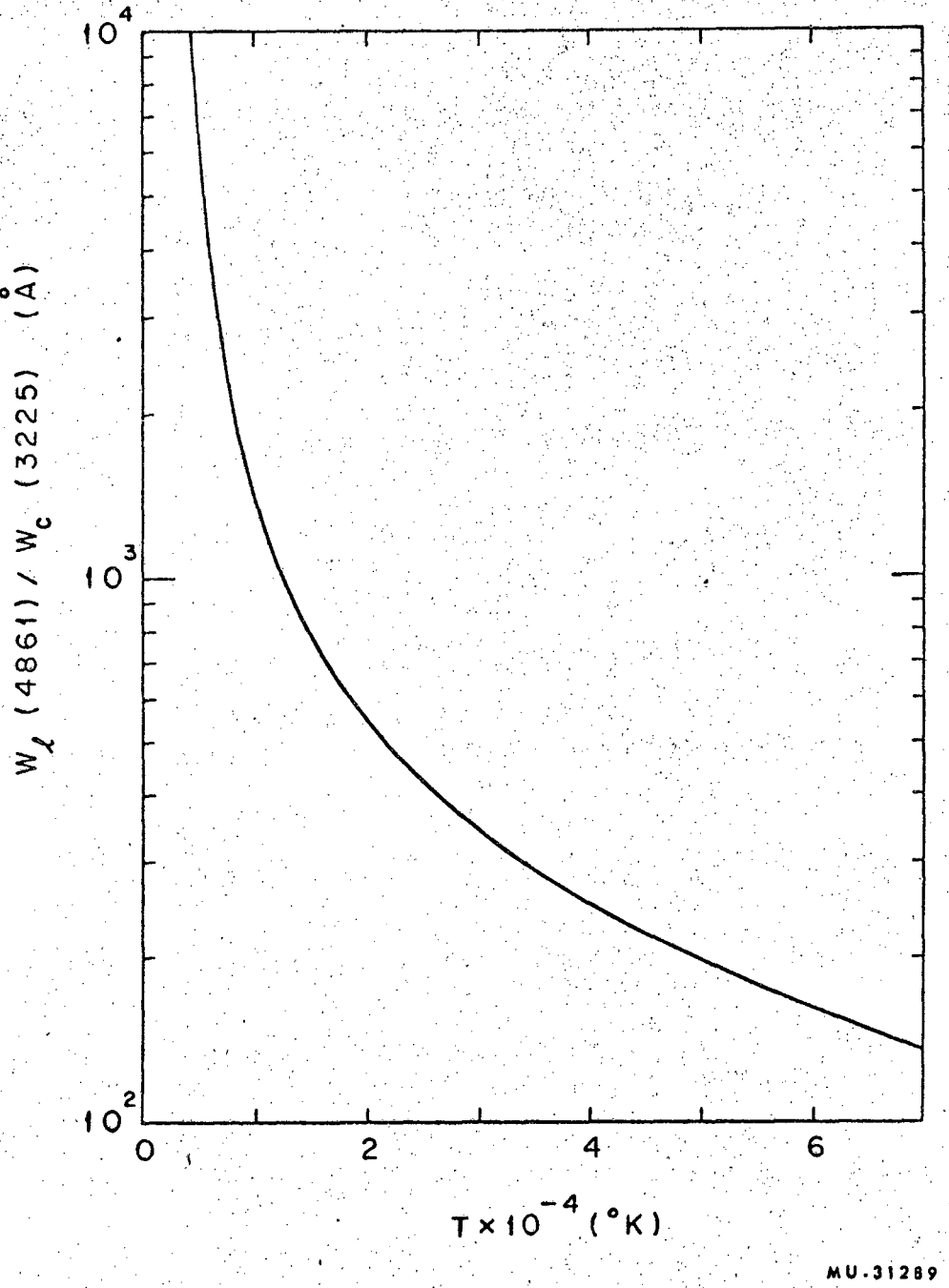

Fig. 8. Plot of $W_\ell(4861)/W_c(3225)$ as a function of temperature.

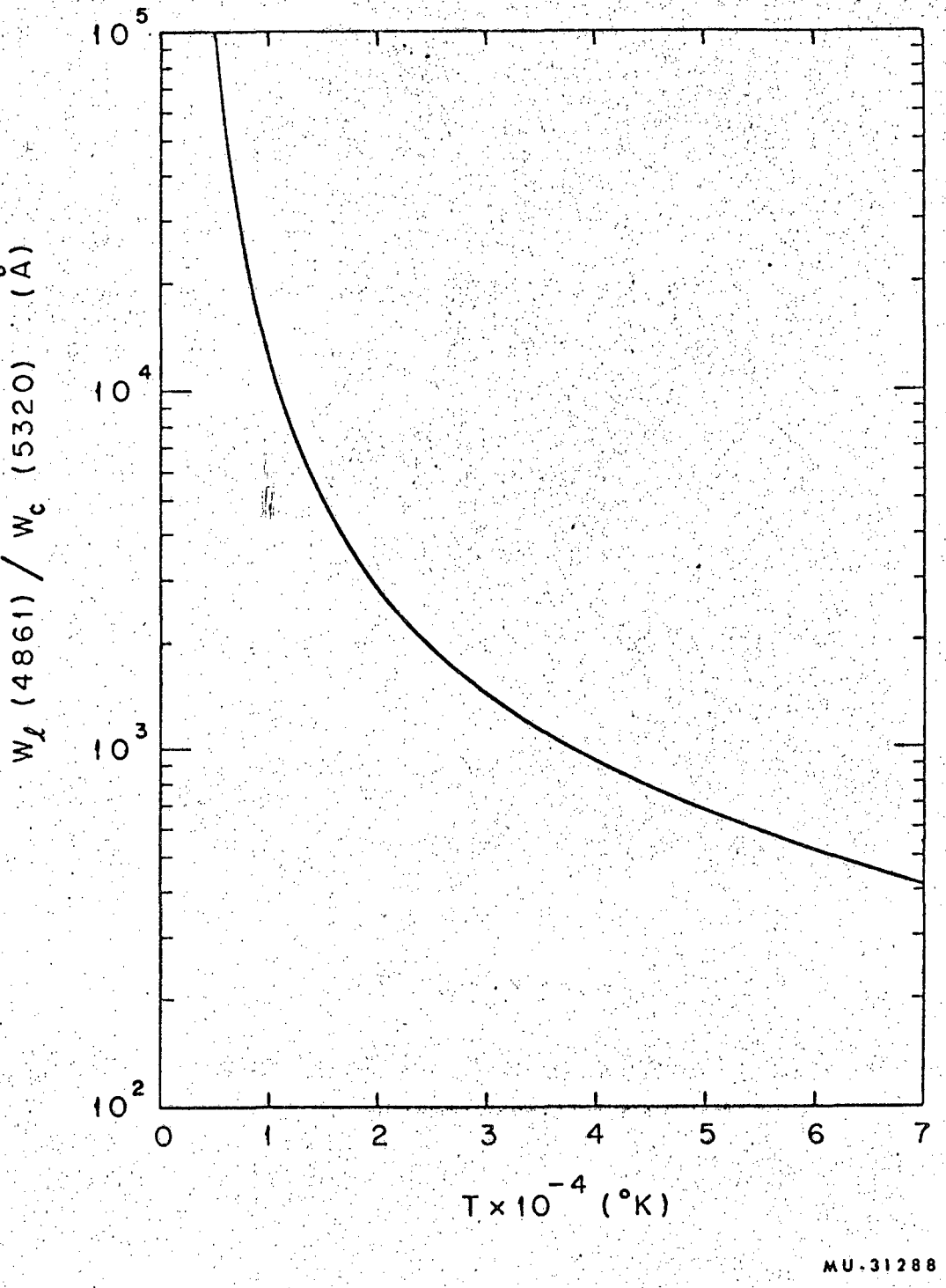

Fig. 9. Plot of $W_\ell(4861)/W_c(5320)$ as a function of temperature.

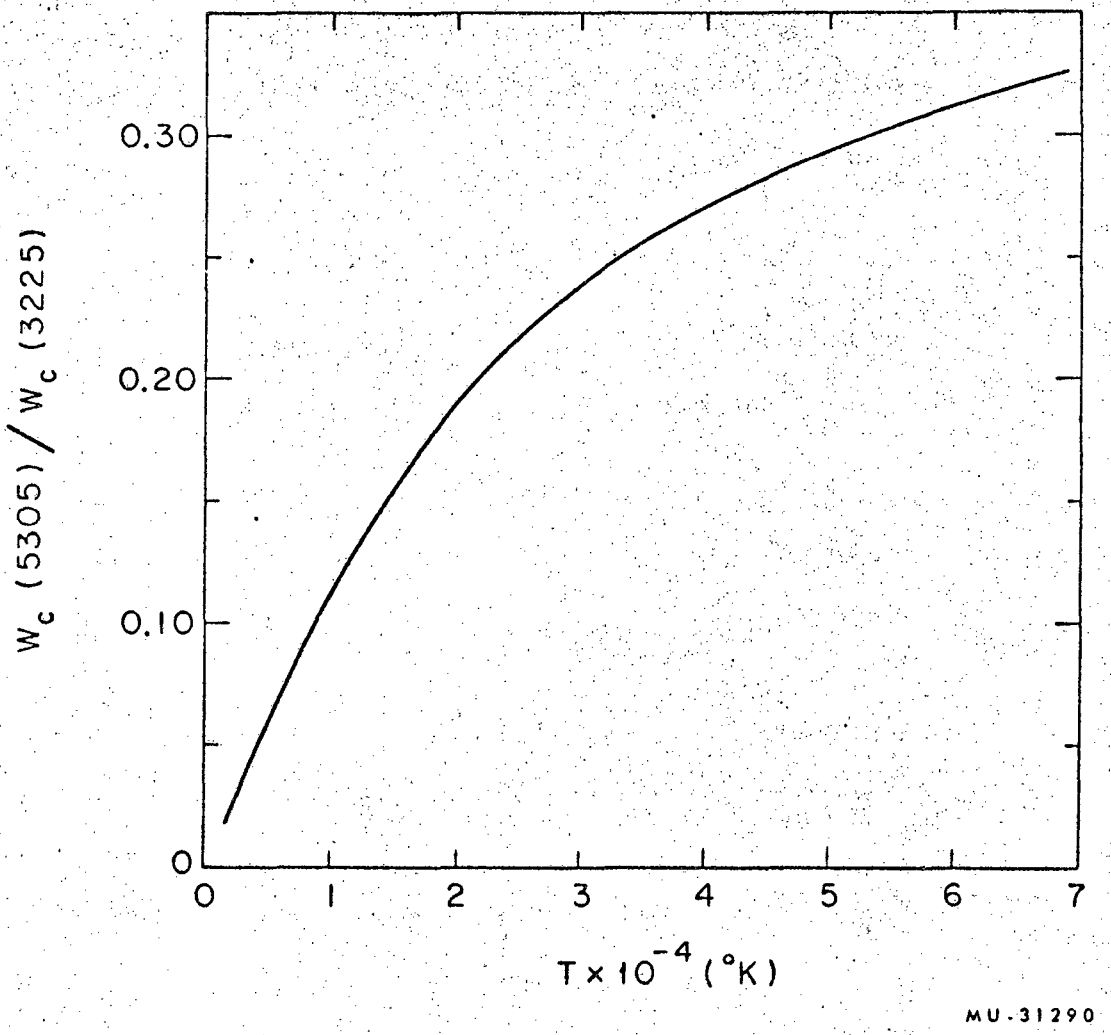

Fig. 10. Plot of $W_c(5320)/W_c(3225)$ as a function of temperature.

III. EQUIPMENT AND PROCEDURES

A. Plasma Device

The experimental device used to produce the plasma has been extensively described in a number of publications.[2,27,28] The following description is intended only as a guide to the reader and to update the description to include the few minor changes required to perform the vacuum uv work.

A hydrogen plasma is produced in a copper cylinder 14.6 cm in diameter closed at one end by a quartz end plate and at the other by a movable copper plate. To assure good electrical contact of the copper plate with the cylinder wall, it was fitted with finger stock around its circumference. This movable copper plate or "plug" was one of the necessary modifications of the basic machine. The maximum length of the machine is 86.4 cm. The plasma chamber is inside a solenoid that produces a uniform dc magnetic field of 16 kG (see Fig. 11).

A base pressure of 2×10^{-5} torr is maintained in the tube. While the experiment is in progress, hydrogen gas flows through the tube, maintaining a pressure of 0.085 torr. While the plasma chamber is maintained at this pressure the two 6-in. (silicone oil) diffusion pumps maintaim the differential pumping sections at a pressure of 2×10^{-5} torr, the pressure differential being across the 1/16 in.-diam holes in the end plates. These two differential pumping sections were the other necessary modification to the basic machine described in previous publications.

A lumped-constant pulse line initially charged to 10 kV is connected by an ignitron switch to the 5-cm-long, 5-cm-diam cylindrical molybdenum electrode which is mounted in the center of the quartz plate. When the ignitron is fired, the gas breaks down and a current of 6.5 kA flows between the electrode and the tube wall. The molybdenum electrode is the anode. This radial current crossed with the uniform axial magnetic field exerts an azimuthal body force on the plasma, causing it to rotate. This rotation produces a back emf

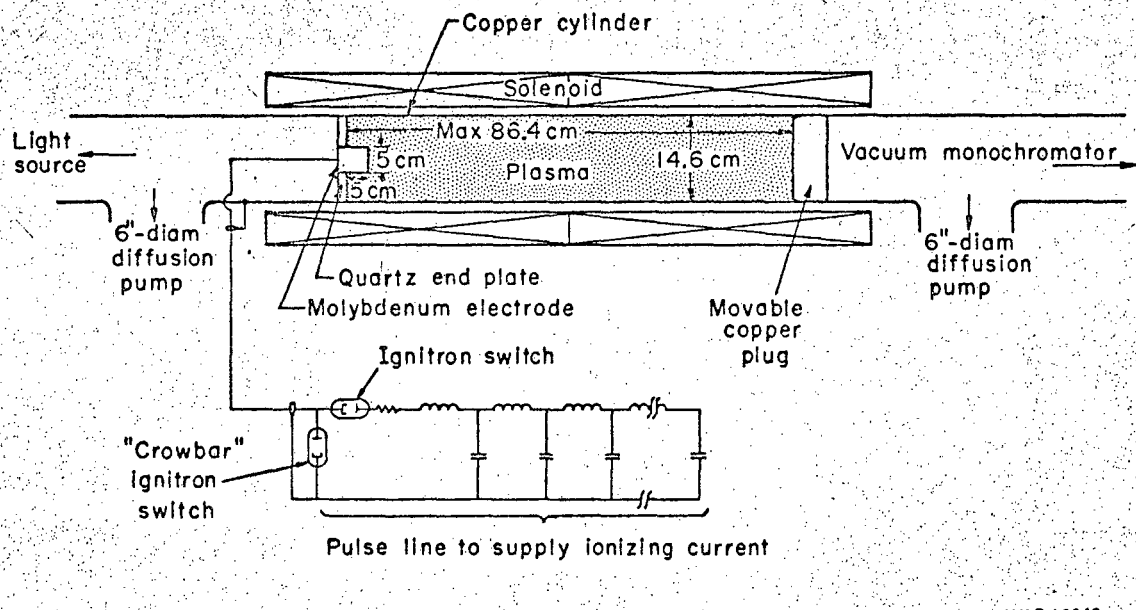

Fig. 11. Schematic drawing of the apparatus used to produce the hydrogen plasma.

forcing the current to flow in the un-ionized region ahead of the rotating plasma. In this way a "hydromagnetic ionizing wave" is produced which has been investigated theoretically by Kunkel and Gross[29] and by Taussig.[30]

If the current is allowed to continue flowing after this front has reached the far end of the tube, prominent spectral lines of impurities appear; therefore, the driving current is "crowbarred", i.e., the molybdenum electrode is shorted to the cylinder wall just as the ionizing wave reaches the far end. This crowbarring forces the plasma to stop rotating. After about 30 μsec, for the full-length tube, the rotational energy has disappeared and the plasma begins to decay. The current for this ionizing front is monitored by a Rogowski belt[31] placed around one of the cables that connect the electrode to the pulse line. The voltage at the tube is measured by means of a resistive divider. Typical voltage and current traces are shown in Fig. 12.

B. Absorption Measurements

Figure 13 is a schematic drawing of the arrangement that was used in this experiment. The light source, described in the next section, was a vacuum spark. Light emanating from the source passes through the 1/16-in. hole in the quartz end plate. After traversing the plasma it exits through the 1/16-in. hole in the movable copper end plate and is incident upon the entrance slits of the vacuum monochromator. The instrument used was a 1/2-m (Seya Namioka) Jarrell-Ash Model 78-650 vacuum scanning monochromator. To increase the sensitivity, we replaced the original grating by a platinum-coated, 1200-lines/mm Bausch and Lomb grating that was blazed for 700 Å. A thin coating of sodium salicylate was used in conjunction with an EMI 9541B photomultiplier tube as the detector. Sodium salicylate has the property that it fluoresces in the visible range when uv light strikes it. The coating was applied to a 3/16-in.-thick, 2-in.-diam Lucite disk. Good optical contact between the photomultiplier and the disk was assured by filling the void between them with Dow Corning 200 fluid (viscosity of

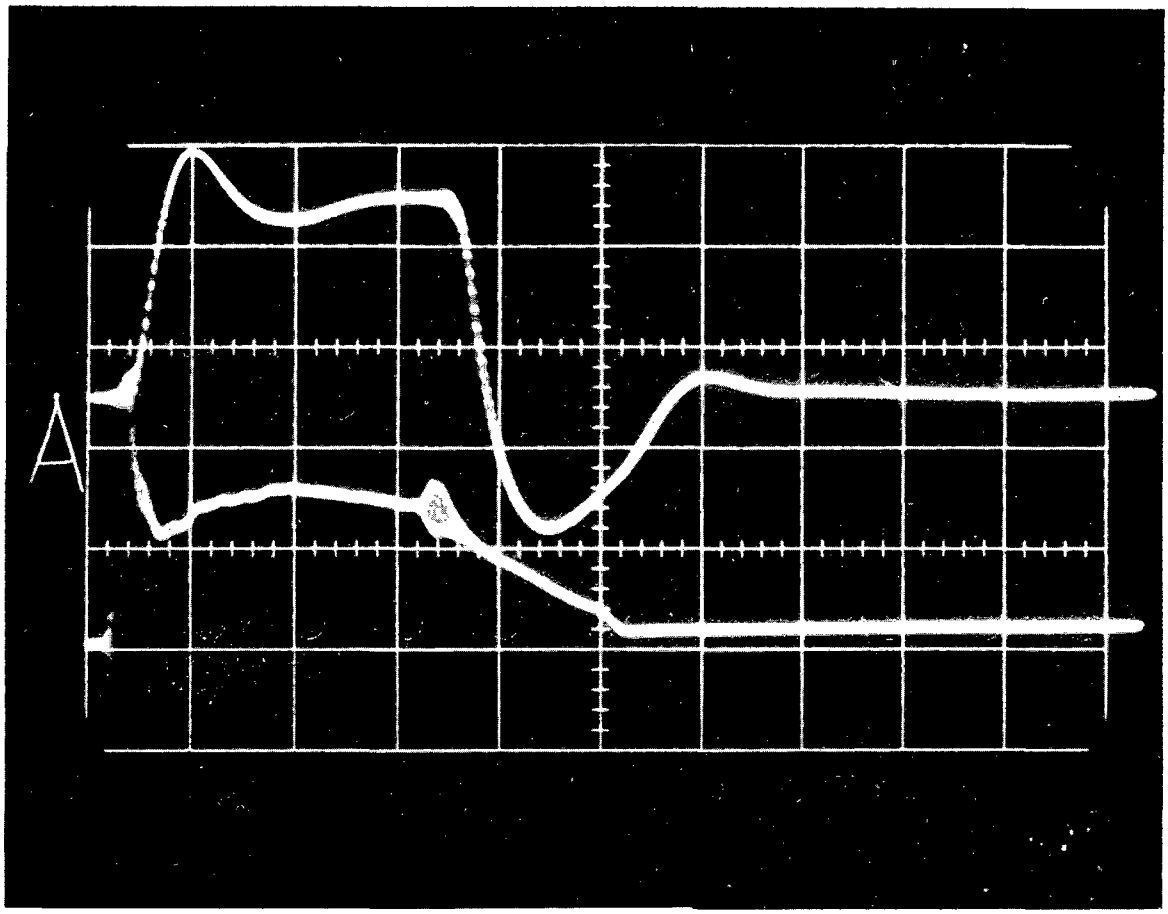

ZN-6008

Fig. 12. Oscilloscope traces of the current (upper) and the voltage of the lumped-constant pulse line used to form the plasma. Sweep is 5 μsec/cm.

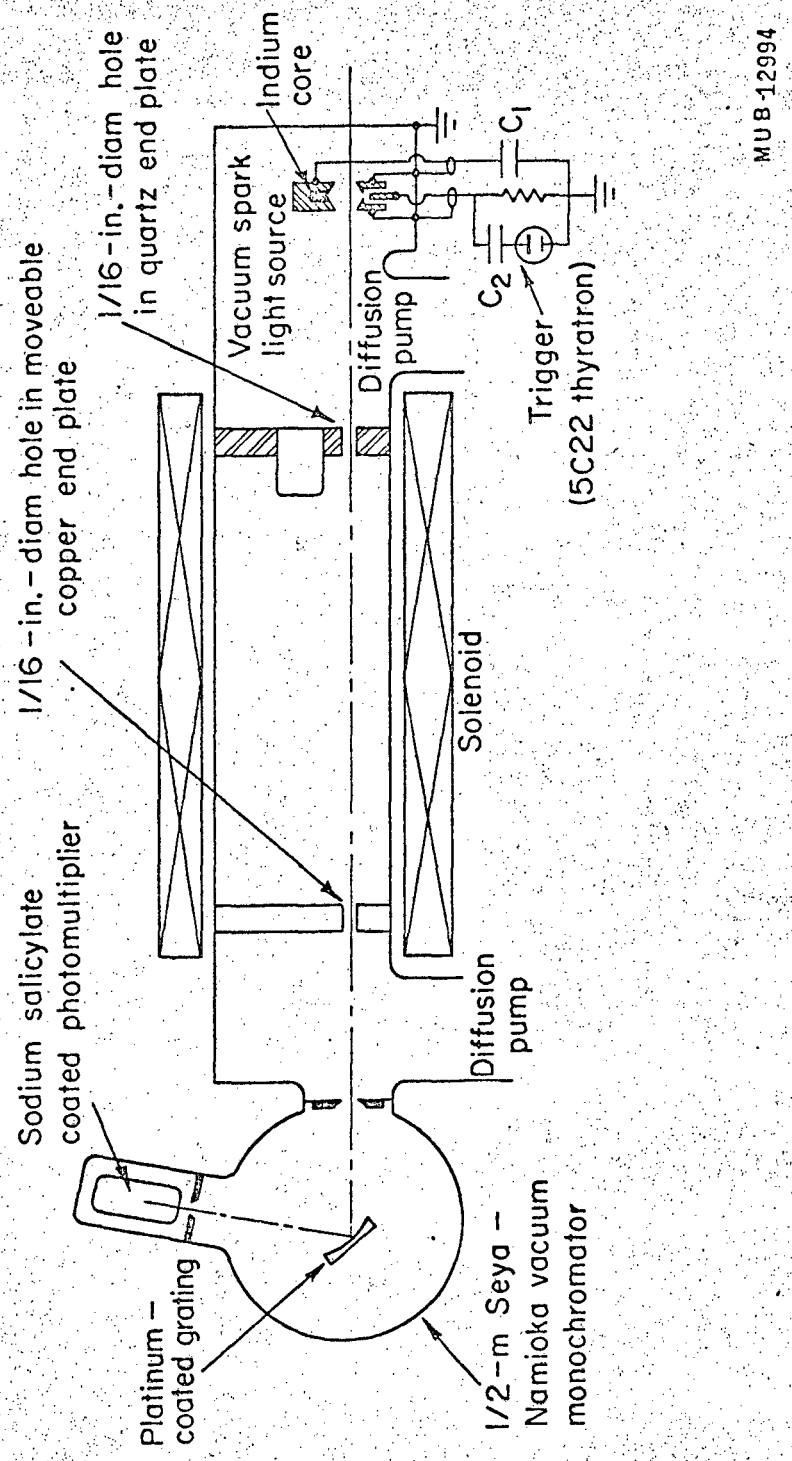

Fig. 13. Schematic drawing of the arrangement used for the vacuum uv absorption measurements.

1 000 000 centistokes). The salicylate coating was applied to a density of about 6 mg/cm^2 with the aid of a Thayer and Chandler artist's air brush (Model A). By creating a 0.5-M solution of sodium salicylate in methyl alcohol and spraying the disk with this solution a very uniform coating could be obtained. The vacuum monochromator mount and the light source were constructed so that they could be translated horizontally in order to be lined up with holes at different radii. There were holes at radii of 3, 5, and 7 cm in the quartz end plate and in the copper plug. When a hole was not being used for a measurement it was blocked by a quartz or copper plug so that the differential pumping would be more effective.

In operation the plasma chamber is filled to a pressure of 0.085 torr of hydrogen gas and the self-timing mechanism on the control panel is started. The machine then "fires" every 45 sec. The sequence of events is as follows. The magnetic field turns on. Five seconds later the ignitrons connecting the lumped-constant pulse line to the plasma chamber are triggered. If the pulse line is charged, the ionization front is formed, and a plasma is produced. At a time of interest, 0 to 200 μsec later, the light source is fired, and the signal emanating from the 1/16-in. hole in the copper end plate is detected. On the next firing of the machine the pulse line is not charged and no plasma is formed. These shots when there is no plasma formed are called normalizing shots. Each point in Figs. 15, 16, and 17 is the average of from 10 to 15 normalizing shots divided by the average of an equivalent number of plasma shots. The errors indicated are standard deviations. These errors are introduced in part by uncertainty in the intensity of the light source and in part by the plasma itself. One of the criteria for selection of a data point was that the rms deviation of the plasma shots had to be greater than that of the normalizing shots. Another test that was used in selection was that the first few normalizing shots had to equal the last few. For example, if 15 plasma shots and 15 normalizing shots were taken, it was required that the average of the first six normalizing shots

be within one standard deviation of the average of the last six normalizing shots and vice versa. It usually turned out that if one criterion was violated, the other was too.

For each plasma shot the current which produced the plasma was inspected to establish that plasma formation was normal. About 2% of the data was thrown out for this reason.

C. Light Source

The light source that was finally developed for this experiment consisted of a vacuum spark gap. The difficulty in a transmission measurement is that one must know how much light is entering the plasma in order that the measured emerging light has any significance. A number of schemes were attempted to monitor the light entering the plasma, but they were all to no avail. This was the result of three factors: (1) One must work in the vacuum uv. (2) The plasma upon which the experiment was to be performed was itself a rather good source of light in the region 860 to 912 Å. (3) The plasma was physically large and required a strong magnetic field. The existence of the magnetic field required that the light source and the light detector be removed somewhat from the experiment proper in order that they function properly. The net result was that the detector was viewing very small solid angles. Unfortunately the light source must of necessity subtend an equal or smaller solid angle than the plasma.

The main attempts at "monitoring" the light source were:

(1) Trying to correlate the current to the light source with its light output.

(2) Using a vacuum monochromator as a light source and monitoring the light coming out the exit slit. This setup was used with two detecting schems: (a) a second vacuum monochromator as a detector, and (b) and 800-Å free-standing film of indium as a vacuum light filter. Both of these attempts were unsuccessful because the plasma was far brighter than the source after dispersion by the monochromator.

(3) Monitoring the light source by a branching-ratio technique.

The indium-III line that was used for this experiment was originally chosen because the 890.84 Å transition is accompanied by a transition from the same upper state that is in the visible. The decay scheme is shown in Fig. 14.

An attempt to monitor the source by tracking the discharge with a separate monomchromator set on one of these visible wavelengths proved unsuccessful. Possibly the problem was one of optics, i.e., the two different monochromators were not viewing the same part of the source. This could be overcome by modifying the vacuum monochromator so that it is a duochromator. It is not clear that this method still could not be made to work. Fortunately, it was noticed that the first three peaks of the existing light source were reproducible enough (from shot to shot) that the experiment could be performed without monitoring the light entering the plasma.

An oscilloscope trace of the observed light signal along with a current trace is shown in Fig. 15. The light source was subject to a number of maladies. After about 300 shots the Kovar vacuum seal of the trigger electrode became sufficiently coated that it began to conduct and the source would not fire. This was easily repaired by removing and cleaning it. A requirement for satisfactory operation was that the 6-μF capacitor C_1 (Fig. 13) had to be charged to at least 14 kV before the source would run reproducibly. Considerable time and effort were wasted before this fact was discovered. After many hundreds of shots the 1/16-in. hole that was filled with indium eroded to the point where it was about 1/8 in. in diameter. At this point the source became very erratic, and new carbon electrodes were necessary. At the beginning of a run the source had to be "warmed up" by firing it about 20 to 30 times. Occasionally for no apparent reason, the source did not run reproducibly. This was usually solved by firing the source repeatedly until it corrected itself.

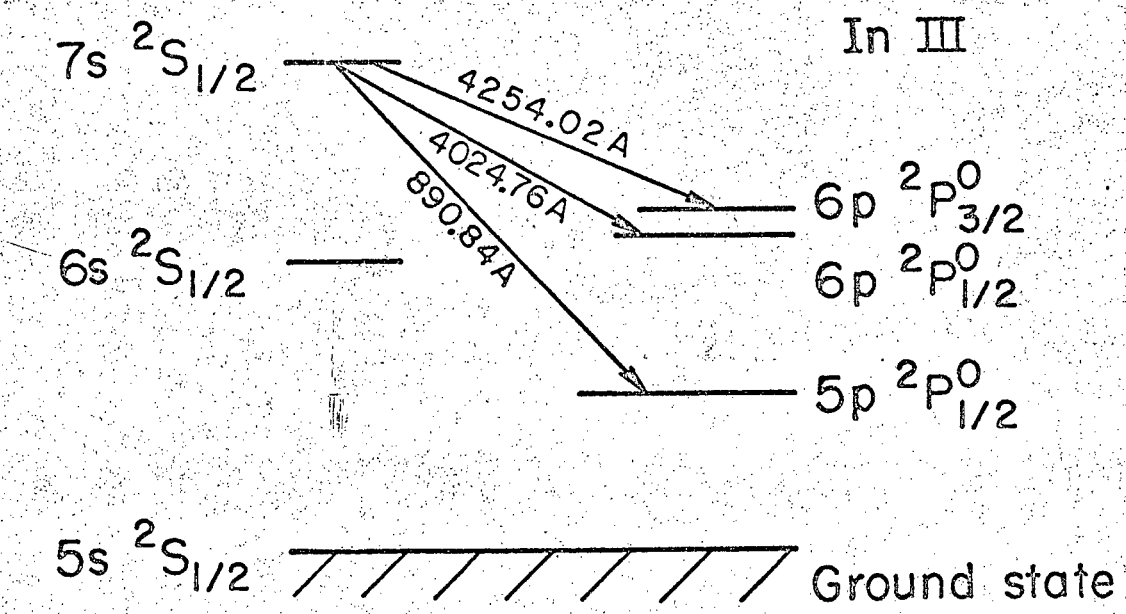

Fig. 14. Partial decay scheme for Indium III.

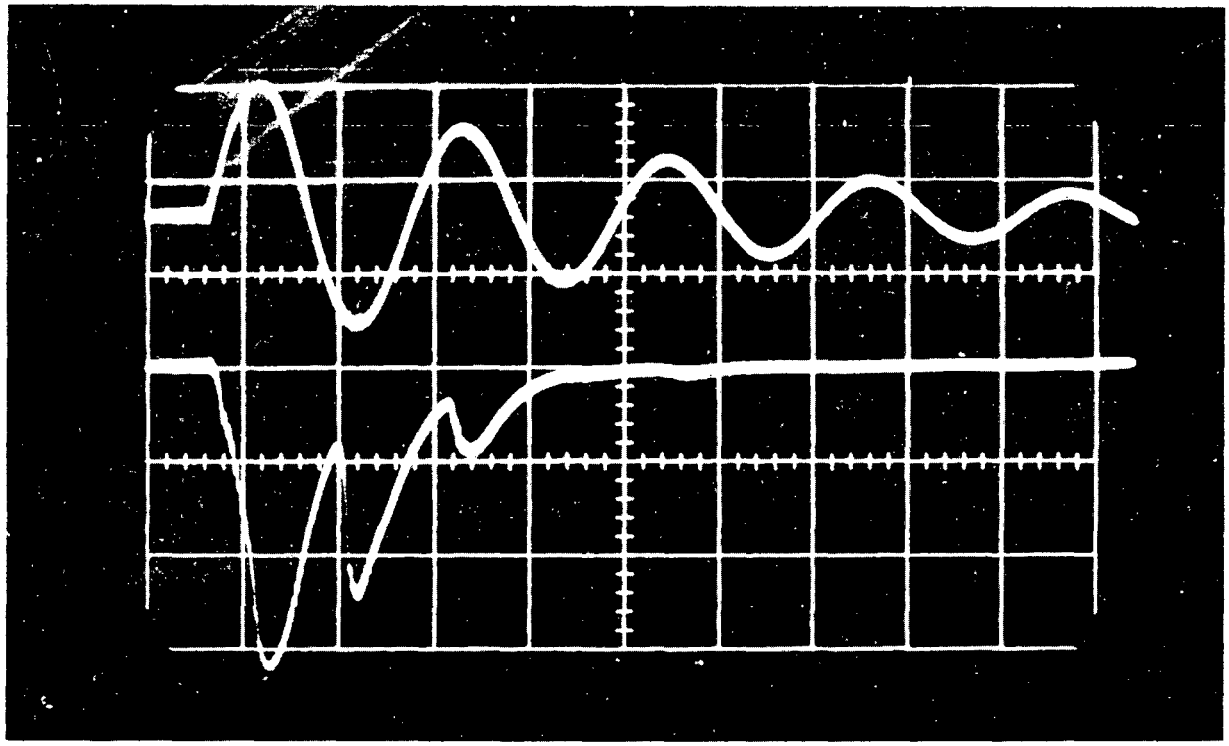

ZN-6009

Fig. 15. Oscilloscope traces of the ringing current to the light source and the light output. The sweep speed is 5 μsec/cm.

D. Visible and Near-Ultraviolt Measurements

The method used for the ion density and temperature followed closely the work of Cooper.[2,28] Based on the theoretical considerations outlined in IIC, the temperature was deduced from intensity ratios and the density was inferred from an absolute-intensity measurement. The actual choices of wavelengths used for the electron temperature and density measurements were governed by a number of factors. A wavelength of 5350 Å was selected because it has a particularly weak temperature dependence. An absolute measure of the radiated light at this wavelength gives a rather reliable measure of the electron density. Across the Balmer series limit from 5305 Å, 3225 Å was chosen because of its strong temperature dependence; hence it should yield accurate temperature measurements. Both regions were also chosen so as to coincide with regions of the spectrum known to be free of impurity lines in the particular plasma that was studied, and also sufficiently far from any Stark-broadened hydrogen line.

We chose H_β (4861 Å) as a line to observe, because it is in a particularly easy region of the spectrum to measure and, for the plasma under investigation, the fourth level was expected to be in Saha equilibrium. The bandwidths chosen were 11.5 Å for 5305 Å, 4 Å for 3225 Å, and 50 Å for 4861 Å. The large band pass for the line was necessary in order to include the wings of the line which is Stark-broadened.

The experimental arrangement is shown in Fig. 16. Radiation leaving the plasma is limited by a 1/4-in.-diam aperture (a quartz window) at the far end of the differential pumping section. It is reflected by a movable front-surface mirror and focused by a quartz lens onto the entrance slit of a Jarrel-Ash Model JA-7102 3.4-meter plane-grating spectrograph. The system was accurately aligned so that the optical axis of the spectrograph was parallel to the axis of the plasma chamber at the same radius as the atomic-density measurements. This was accomplished with the aid of a helium-neon gas laser.

Located in the focal plane of the spectrograph were three movable assemblies. Each assembly contained an adjustable exit slit and an EMI 6255B photomultiplier tube with its associated wiring. Each tube

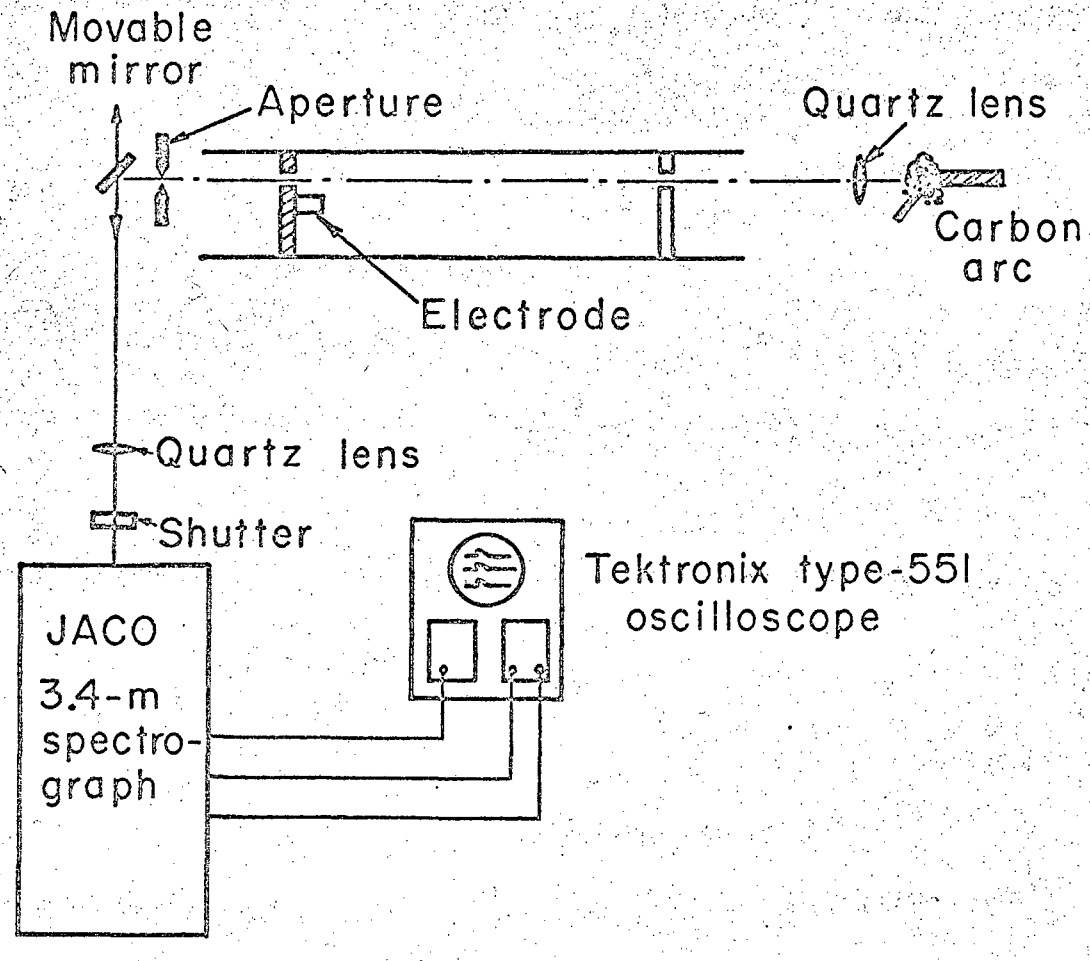

MUB-13840

Fig. 16. Schematic drawing of the equipment used in making the "visible" spectroscopic measurements.

was shielded from the stray magnetic field associated with the experiment by a mu-metal shield enclosed in two concentric soft-iron cylinders. Even with the shielding there is still an effect on the tubes from the magnetic field of the experiment. The tubes were rotated about their axis until this effect was minimized and then the remaining effect, about 2%, was included in the reduction of the data.

To cut down on scattered light and to eliminate overlapping orders (3225 Å was observed in second order), filters were placed in front of the photomultipliers. Interference filters were used in the visible range and a Corning type 4-76 ultraviolet filter was used for the observation at 3225 Å.

For calibration the machine was let up to air and the copper plug (end plate) removed. The anode spot of the carbon arc was focused by a quartz lens on the quartz window (aperture). This effectively replaces the plasma with the image of the anode spot. A camera shutter was employed to give a 4-msec light pulse with a 200-μsec rise time. A light pulse was used rather than a steady source so as to simulate the experiment better. Without this precaution the capacitors shunting the last few dynodes would have discharged somewhat, resulting in errors of calibration. These capacitors were chosen so that the gain change was less than 2%/msec for viewing a pulsed light source which created an anode current of 1 mA. No signal from the plasma or the arc exceeded this value.

To eliminate errors due to drifts in gain of the photomultipliers, we used a secondary standard. Mounted within the spectrograph is an Ar-4 argon lamp. A small pulser connects a delay line charged by a very stable dc power supply. This source gives sixty 50-nsec light pulses per second. The device was developed for similar use by the Counting Research Group at this laboratory.[32] The temperature coefficient of this light is 0.1%/°C. The procedure employed in making the temperature and electron-density measurements was as follows.

The apparatus was checked to determine that everything was in working order. The gains of the three photomultipliers were checked

against the argon lamp. Measurements of the plasma were performed, taking about 10 min, and the gains of the photomultipliers were again checked against the argon lamp. The machine was then let up to dry nitrogen, and the carbon arc was set in place. The anode spot of the arc was focused upon the aperture and the gains of the photomultipliers were again checked against the argon lamp. Usually there was no observable change in gain during the 1/2 hour necessary for the setup of the arc. The arc was then run, and the photomultipliers calibrated. Once again the argon lamp was employed. Occasionally a very slight drift could be detected, and this was corrected by changing the voltage on that particular photomultiplier by a volt or two.

The equipment used for the electron-temperature and density measurements is the same equipment used by Cooper.[2,28] For more detailed information concerning the equipment and reasons for choosing particular components see reference 2.

IV. RESULTS

A. Discussion

Absorption measurements were made at radii of 3, 5, and 7 cm. For the 3- and 5-cm measurements it was possible to vary the length of the plasma. The construction of the movable plug (copper end plate) unfortunately precluded changing the length for the 7-cm radius. The observed attenuation at this radius is very different than at the other two during the time that the front is coming down the tube. Whereas the attenuation is constant during the first 20 to 30 μsec for the smaller radii shots, there is an essentially linear increase in $\ln I_0/I$ for the shots near the wall. This was interpreted as the formation of a layer of neutral atoms near the wall while the front is progressing. Therefore it was felt that it would be reasonably safe to interpret the absorption at this length as directly due to neutrals along the entire length, assuming no end effects. Figures 17, 18, and 19 show the observed absorption for the three radii. The ionizing front that produces the plasma proceeds down the tube at a rate of about 5 cm per μsec. In order to make a fair comparison between the 63.5-cm data and the 86.4-cm data, the two were matched at the time when the reverse current of the slow bank went through zero. (This time is 32 μsec in Fig. 12.) The time scale in these figures is that of the 86.4-cm data, the 63.5 having had the appropriate shift. Figures 20, 21, and 22 are plots of the atomic and electronic densities and their sum for the three radii. Several features should be noted. For the 3-cm position the plasma does in fact recombine *in situ*. One can see from Fig. 23 that the plasma in this region obeys Saha's equation up to a time of at least 200 μsec. The fact that the observed absorption is independent of the plasma length for early times (at both 3 and 5 cm) is direct evidence that this plasma is initially highly ionized. The time behavior of the total density at the two outer radii shows that there is a layer of atomic hydrogen formed at the wall and that this layer moves in radially in time. This is more easily seen in Figs. 31 and 32 of Appendix D.

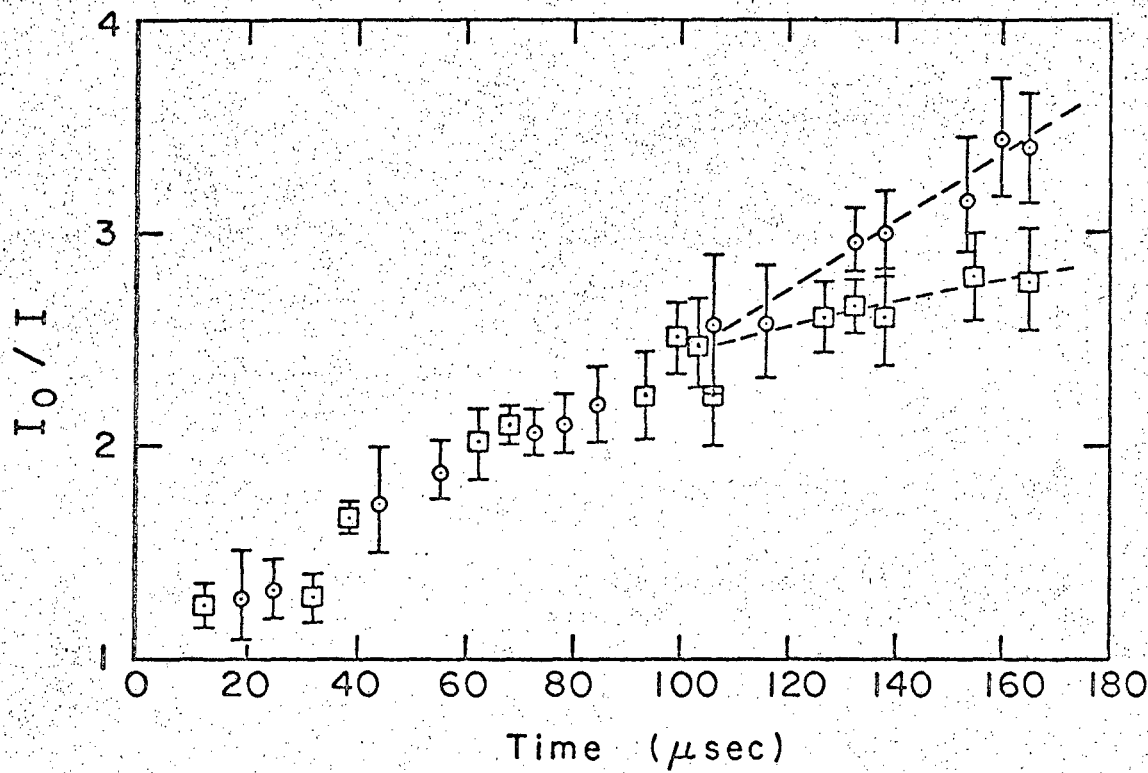

Fig. 17. Measured absorption for the two lengths at a radius of 3 cm. The length of the plasma is 86.4 cm for the circle data and 63.5 cm for the square data points.

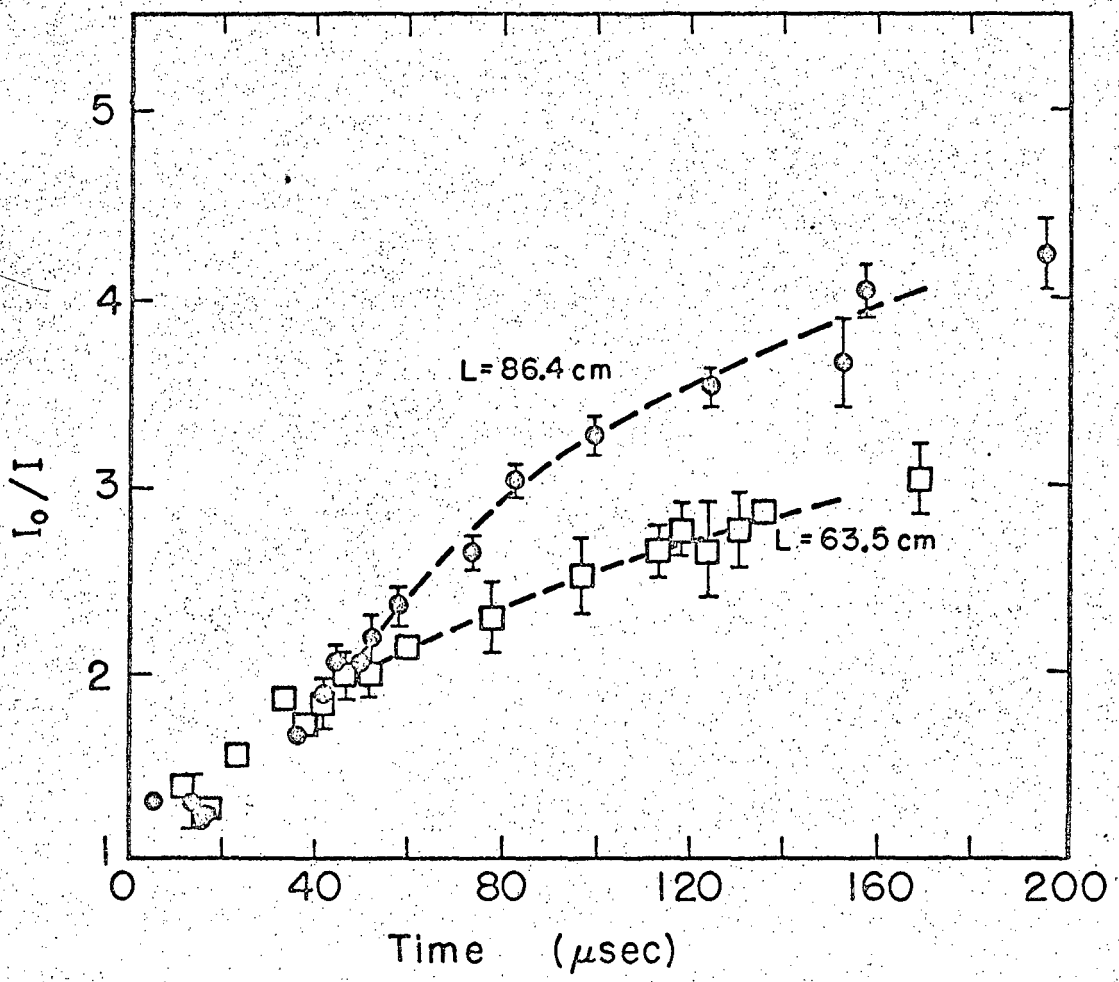

MUB-13838

Fig. 18. Measured absorption for the two lengths at a radius of 5 cm.

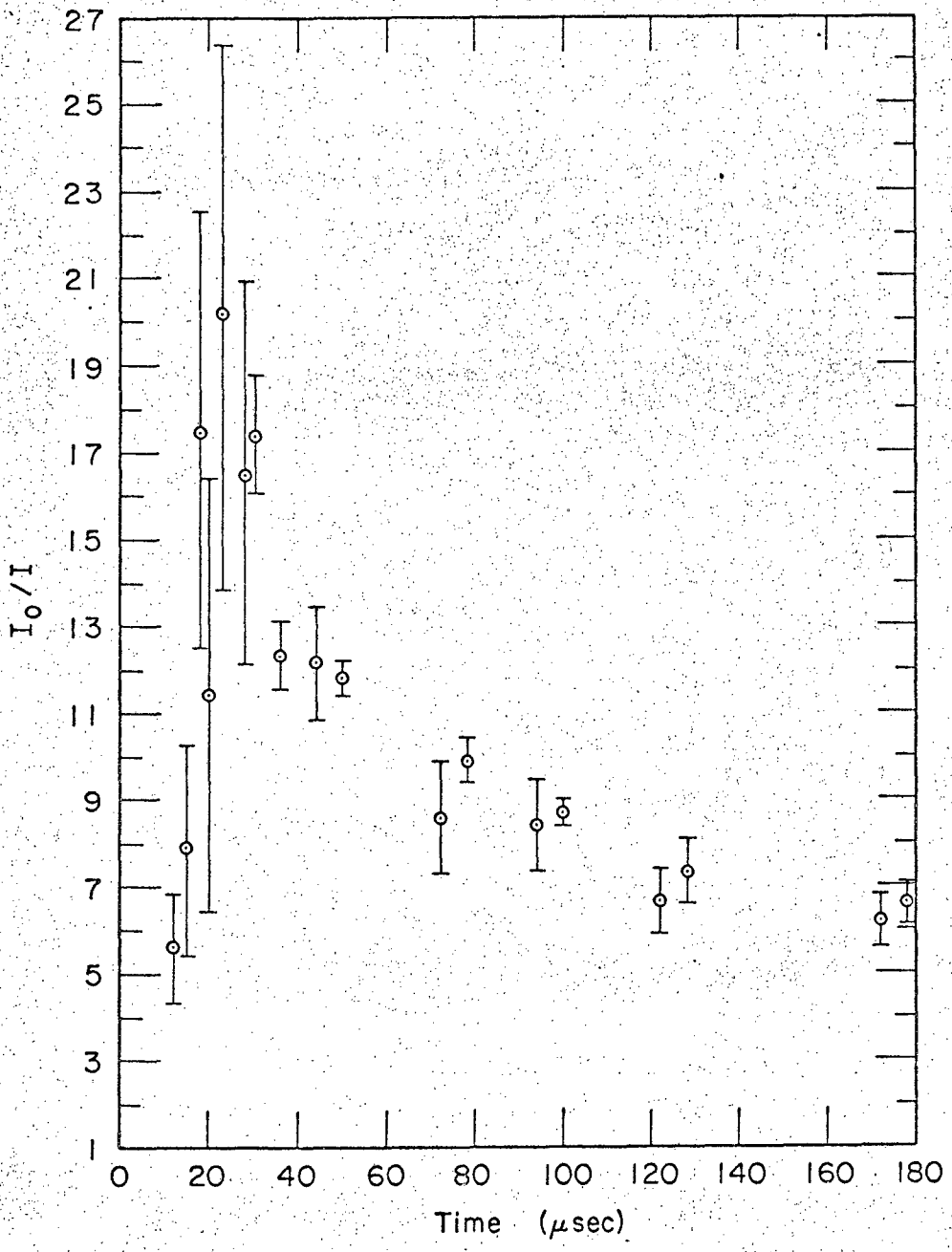

MUB 13000

Fig. 19. Absorption measurements at the 70cm radius. (L = 86.4 cm.)

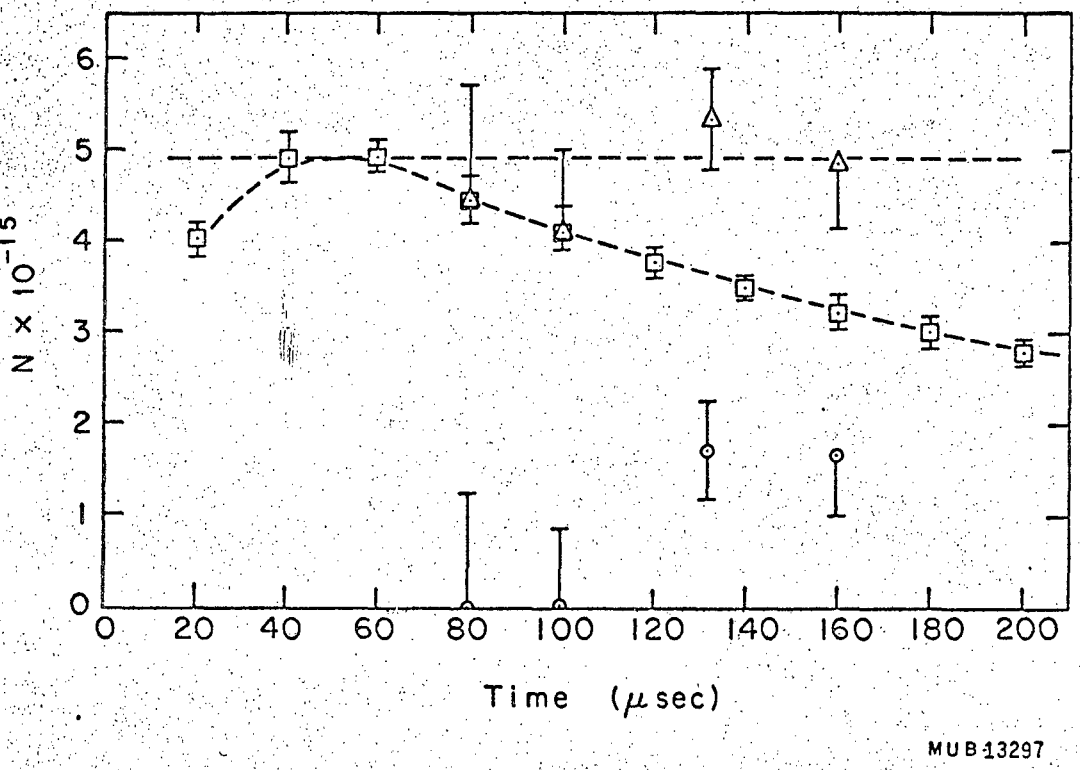

Fig. 20. Densities as a function of time for the 3-cm radius. Circles are the atomic density, squares the electron density, and triangles the sum of the electron and atom densities.

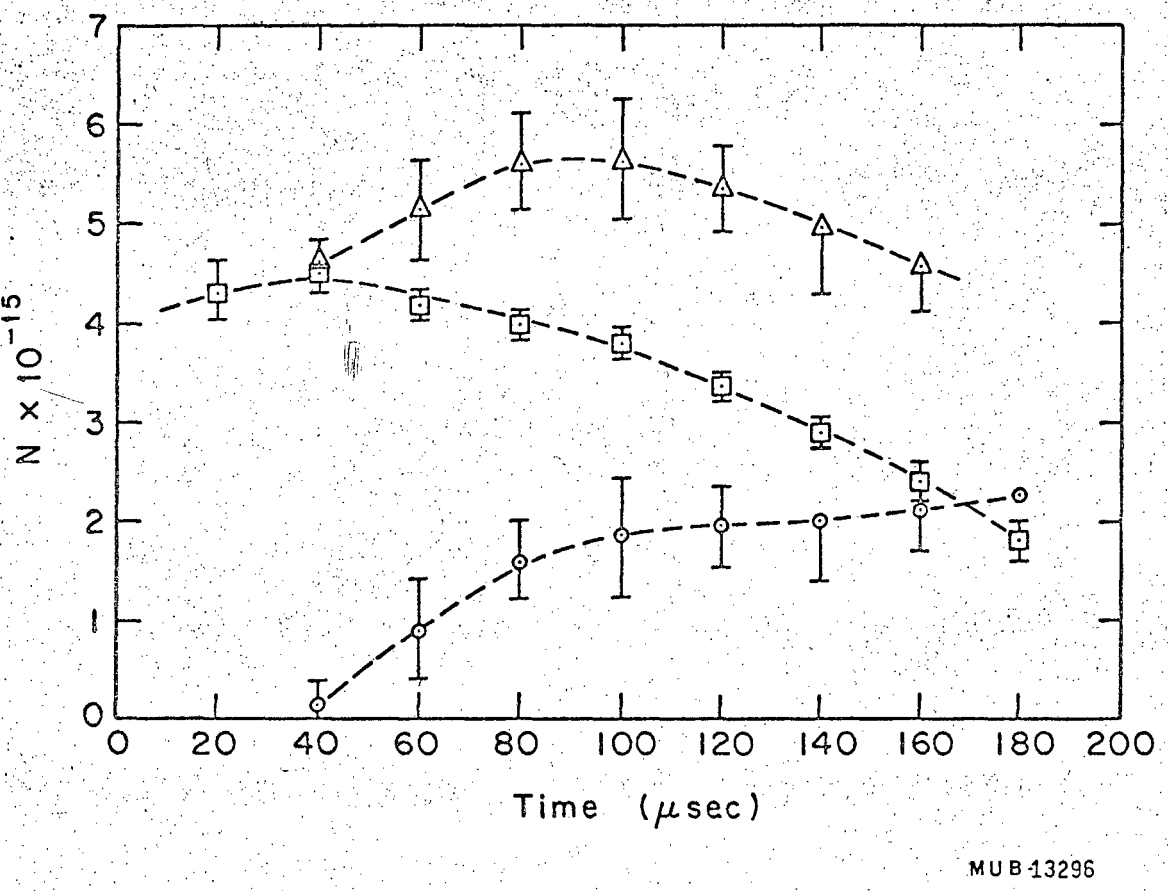

Fig. 21. Densities as a function of time for the 5-cm radius. Circles are the atomic density, squares the electron density and triangles the sum of the electron and atom densities.

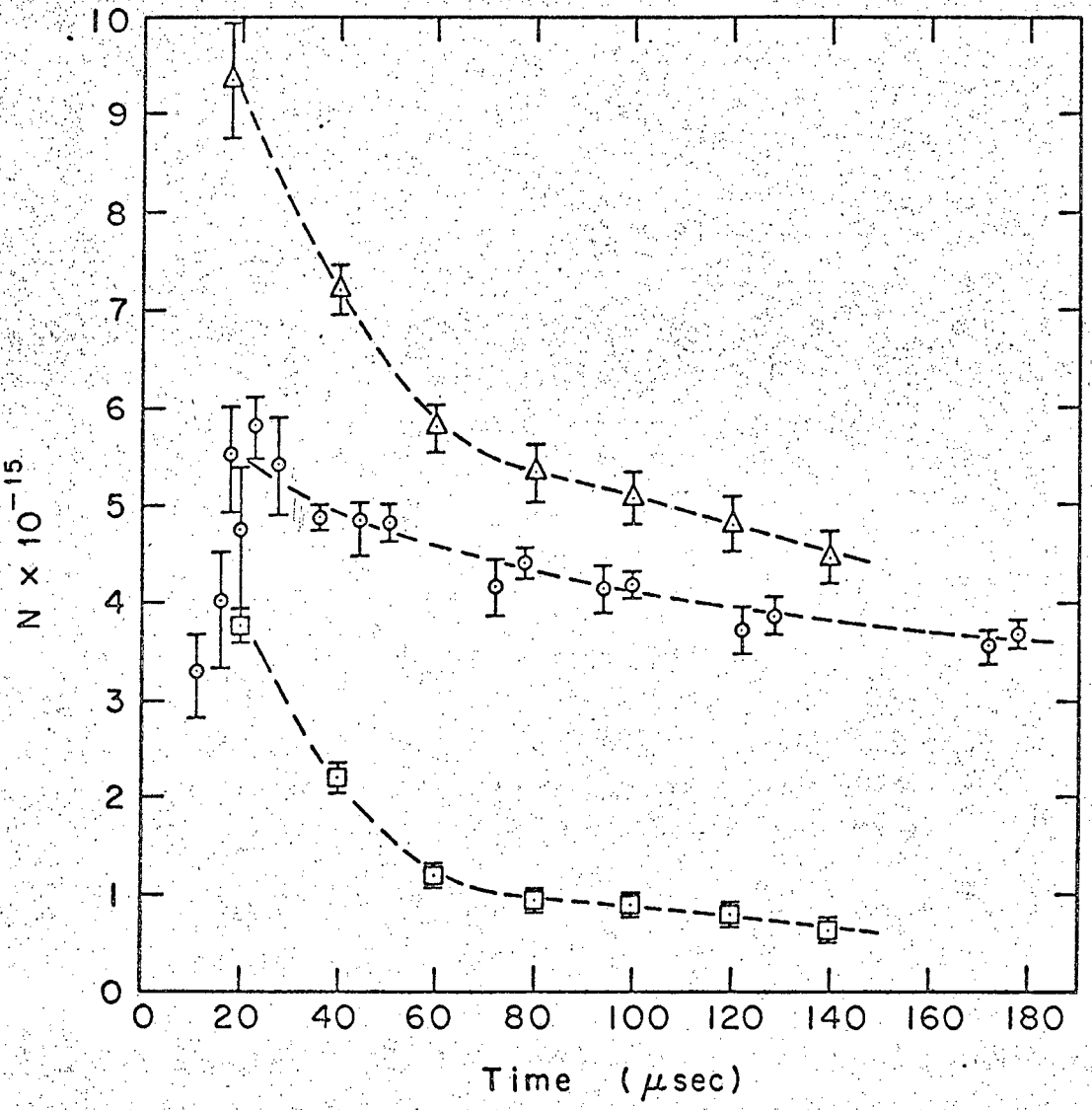

Fig. 22. Densities as a function of time for the 7-cm radius. Circles are the atomic density, squares the electron density, and triangles the sum of the electron and atom densities.

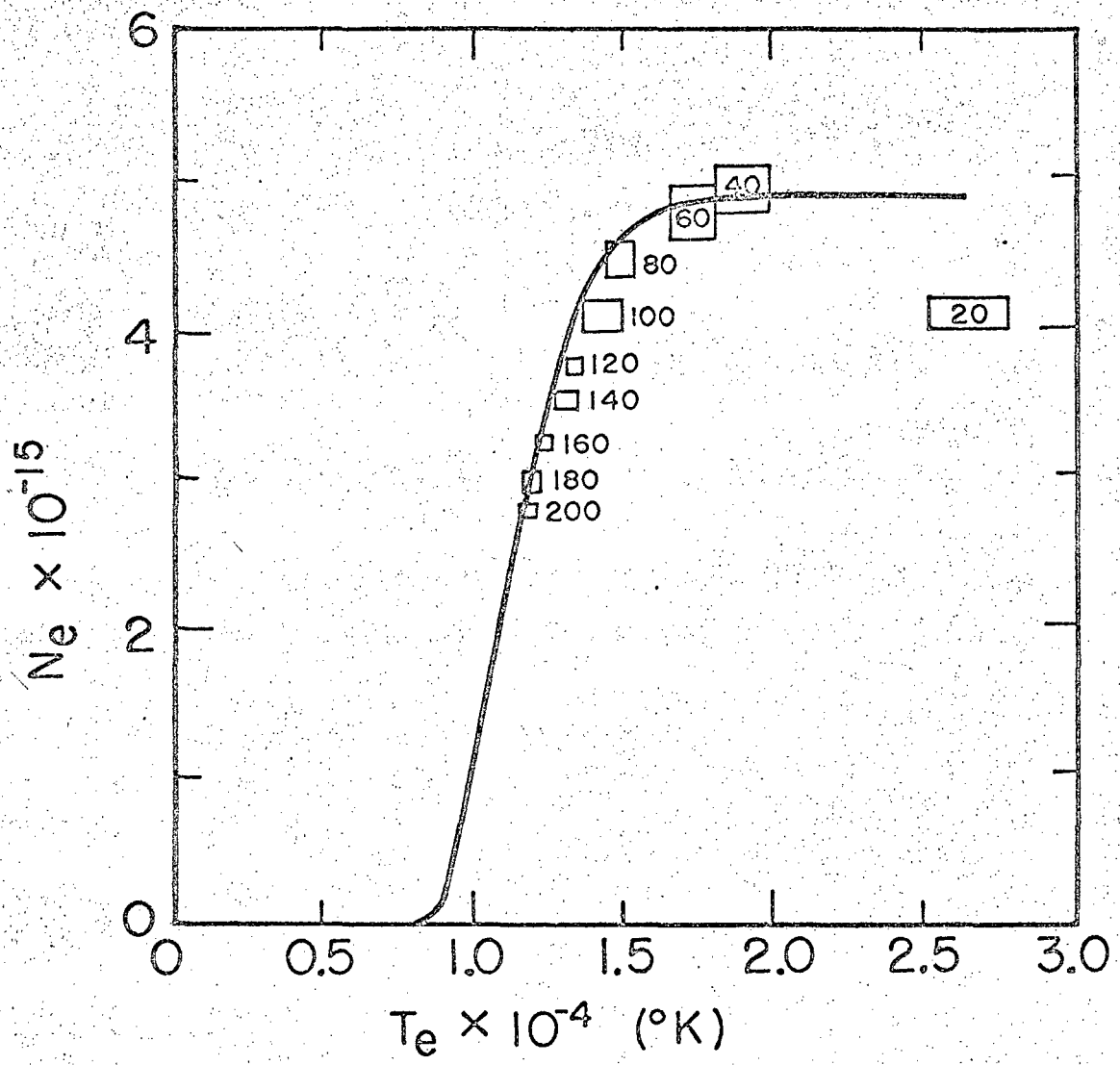

MUB-13839

Fig. 23. Plot of the observed electron density vs the observed electron temperature for various times during the decay. The data is for the 3-cm radius. The solid line is Saha's equation normalized to an electron density of 4.9×10^{15}.

The plasma is rotating during the time that the front is coming down the tube because of the $\underline{j} \times \underline{B}$ force. It is not difficult to imagine processes that could form such an atomic layer at the wall.

In considering the possible ways that the atomic hydrogen near the wall can get into the central portions of the plasma, the first thing to do is to roughly estimate the diffusion time due to charge exchange. For a rough model consider the ions to be tied to the magnetic-field lines. The neutrals will obey the diffusion equation

$$\frac{\partial N_0}{\partial t} = - \nabla \cdot D \nabla N_0, \tag{31}$$

which may be crudely approximated by

$$\dot{N}_0 \approx - \frac{D}{\Lambda^2} N_0.$$

If we assume that the atomic density decays as $e^{-t/\tau}$, the τ equals $\tau \simeq \Lambda^2/D$. For the diffusion coefficient we may use

$$D = \frac{1}{3} \frac{\langle v \rangle}{N_i \sigma} . \tag{32}$$

Assuming value of $N_i \sim 1 \times 10^{15}$, $\sigma \sim 5 \times 10^{-15}$, $\Lambda \sim 2$ cm, and $v \sim 10^6$, we obtain τ of the order of 60 μsec. This is the right order of magnitude to compare with the observed influx. In the actual case there are considerably more complications. The ion density is actually a function of both position and time. The diffusion coefficient then will not commute with the divergence operator, and further the differential diffusion equation may not be solved by the separation-of-variables method. In addition, two mean free paths must be considered. The first is that of charge exchange, and the other that of ionization. Figure 2 is a plot of the ionization coefficient as calculated by Bates et al.[13] The graph was obtained by interpolation of their tables. As can be seen, this ionization coefficient is strongly dependent upon temperature. If the electron temperature is high enough, the mean

free path for ionization will be considerably shorter than that for charge exchange. For electron temperatures above about 12 000°K at electron densities present in this experiment, the ionization process is the more likely. The problem then becomes a rate problem involving the atoms diffusing inward through charge-exchange collisions to a radius where the electron temperature is high enough that ionization takes over, combined with the rate at which the plasma can maintain the electron temperature by conducting energy outward. This is clearly a very complex computational problem. Considering the very limited interest there would be in such a computer calculation, it has been decided to restrict the calculations to the previous very crude estimate.

Upon inspection of the absorption plots, it is apparent that there is considerable absorption early in time even though the plasma proper is fully ionized. This must be attributed to absorption in a boundary layer. This is not too surprising as there must be something holding the plasma in place. The plasma has an ion and electron density of about 4×10^{15}/cc and a temperature of about 1 eV. The quartz and the copper end plates are nearly at room temperature. Somewhere in between the plasma and the end plates there must be a region where the electron density drops off and the atomic density builds up. Visible measurements made looking across the cylinder at various positions along the tube indicate that this transition layer must be less than 1-cm thick. If we assume that the atomic density is zero in the plasma and start 1 cm from the end plate, the atomic density increases linearly to a maximum at the end plate; for the observed attenuation, the atomic density can reach a value of 10^{17}. One of the original questions was where did the 20 to 30% of the original gas filling go? The answer then is elsewhere. A goodly number of atoms are employed maintaining pressure balance at the ends while the rest have been displaced radially.

The central remaining question about this particular plasma is the manner in which it loses its energy. Knowing the ion density as a function of position and time, an estimate of the energy density and

its time rate of change is possible. The observed change in time of this energy density may be equated to the divergence of the product of a thermal gradient (measured) and an effective thermal conductivity,

$$\frac{\partial \epsilon}{\partial t} = - \nabla \cdot K_{eff} \nabla T. \qquad (33)$$

This effective thermal conductivity may be compared with a theoretical conductivity of a mixture of hydrogen atoms and plasma by using the measured atomic and electron densities. The effective thermal conductivity thus calculated is considerably larger than predicted by theory, suggesting that other mechanisms are transporting thermal energy or ions across the magnetic field.

One possible contribution would be anomalous diffusion. If one attributes to anomalous diffusion all of the observed energy loss in excess of that due to normal heat conduction, one obtains a diffusion coefficient over an order of magnitude larger than Bohm's diffusion coefficient as defined in Spitzer.[33] Observed radial density profiles[2,28] moreover would not be consistent with diffusion-controlled decay. In addition the behavior of the total particle density as a function of time shown in Figs. 20 and 21 does not indicate any rapid radial transport of material. One must assume, therefore that other mechanisms are active in the transport of energy.

Energy loss due to radiation is possible. The estimates of Bates et al. on the power radiated by recombining plasmas that are optically thick to the lines of the Lyman series are also too small to account for the observed energy decay. Their calculations, however, assume that there are no gradients in temperature or density. This is definitely not the case in this plasma.

Detailed calculation of the energy loss due to all forms of radiation might account for the observed decay, but at present it must be considered as one of the remaining unknowns of this plasma.

Another possible source of energy loss would be the flow of ions to the ends of the machine. At the end of the machine there is a layer of atoms which is maintaining pressure balance. Because there is a

radial gradient in the plasma particle pressure, there is expected to be a radial pressure gradient within the atomic layer at the ends of the machine. What is maintaining this gradient is not known. It may well be that there is a circulation set up, and that this circulation is indeed contributing appreciably to the energy loss of this plasma. The dependence of the observed decay of the electron density upon the length of the machine is possible evidence that such a situation exists.

B. Errors

Errors could arise in the absorption measurments if light from the plasma contributed significantly to the observed signal. This was the case only when the ionizing current was flowing. After crowbar, the signal due to the source was at least two orders of magnitude greater than that due to the plasma. While the front was coming down the tube, the signal from the plasma only produced a shift in the base line upon which the light source signal was easily distinguishable. Light from the plasma introduced no significant error.

Probably the greatest source of error that would not be averaged out in the data reduction would arise from light scattered within the vacuum monochromator. In order to estimate this error a number of tests were performed. The first and most obvious was to remove the sodium salicylate coating. This made the system insensitive to all radiation below the transmission of Lucite. With maximum gain of the oscilloscope (0.005 V/cm) the electrical noise produced by the firing of the trigger 5C22 produced more signal than scattered visible light. An upper limit for the scattered visible light must then be about 0.5%, which is negligible.

Another test was to fill the plasma chamber with hydrogen to a pressure of 0.9 torr and compare the signal received with those obtained when the pressure was 2×10^{-5} torr. The hydrogen in the chamber would absorb light from about 860 Å on down. Within the uncertainty of the measurements no difference could be observed.

Yet another test was to scan the 890 Å region with the vacuum monochromator. The 890.84 Å In-III line stood out a factor of six

above the continuum signal. Probably the most sensitive test was the experiment itself. At the 7-cm radius at the time of maximum absorption only 5% of the incident light gets through. This sets an upper limit to the scattered-light contribution.

To get some idea as to the validity of the assumption that the decay of the plasma is independent of the plasma length, electron density and temperature were measured as a function of time for both lengths at 3-cm and 5-cm radii. The plasma is undergoing a "phase transition" during the decay; it is changing from the plasma state to the gaseous state. The electron temperature then is not too sensitive a measure of the state of the plasma. The electron-density measurements showed considerably more deviation for the two different lengths than did the temperature measurements. Figures 24 and 25 are plots of the measured electron density for the two radii, 3 and 5 cm, and for the two lengths. The results are that for the 5-cm data there is a significant deviation at about 120 μsec. After this time the assumption simply is not valid. No correction has been made for this in the presentation of the data, because it is not clear how to do it in any consistent manner. The time of deviation for the 3-cm data seems to be later at about 140 μsec. After these times the measured atomic density should be considered as a lower limit.

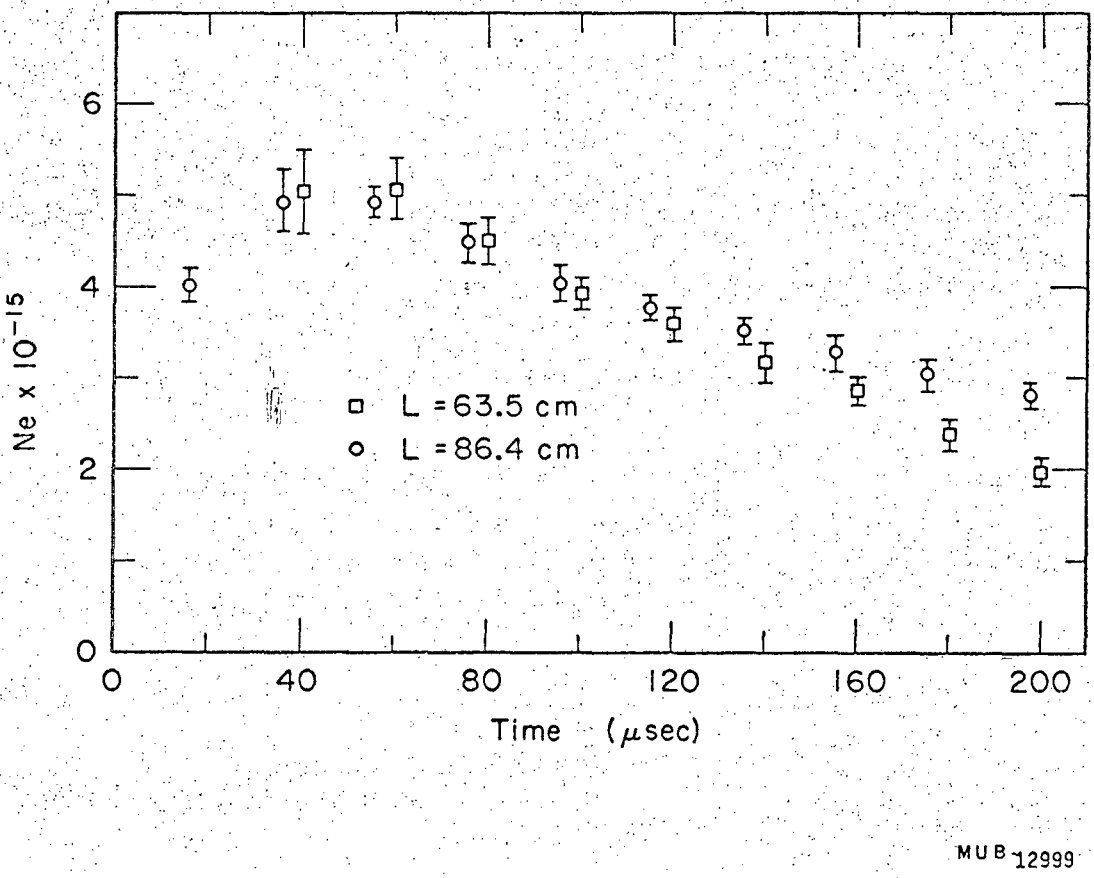

Fig. 24. Electron-density measurements at the 3-cm radius. The circles are the data for the 86.4-cm length, the squares for the 63.5 cm length.

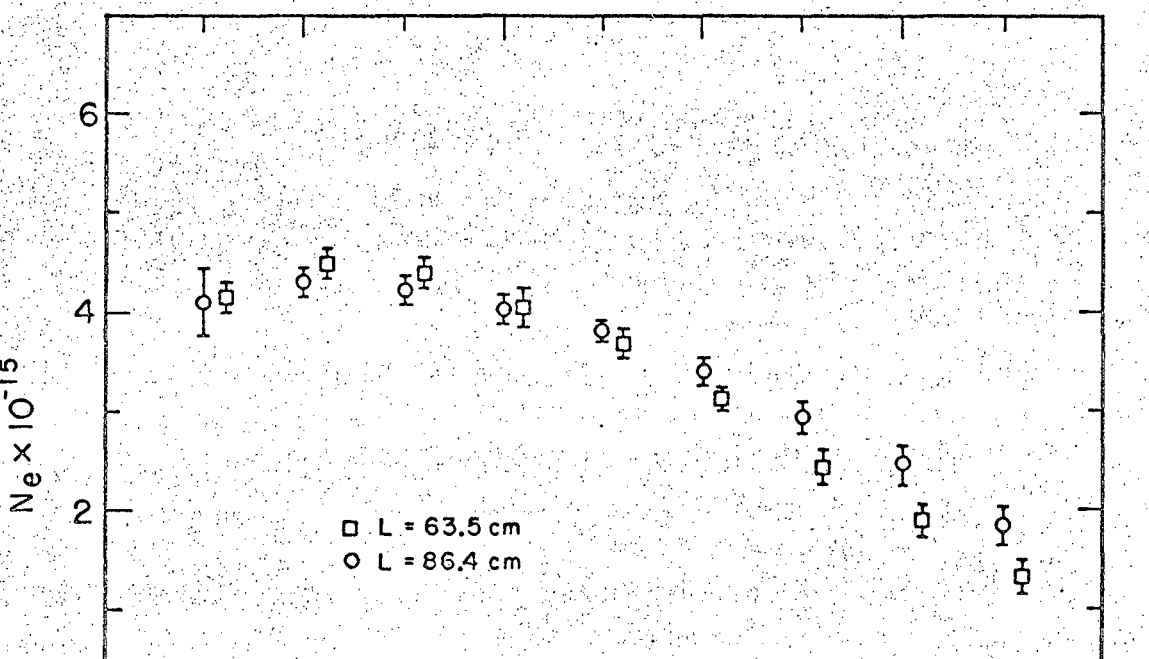

Fig. 25. Electron-density measurements at the 5-cm radius. The circles are the data for the 86.4-cm length, the squares for the 63.5-cm length.

V. CONCLUSIONS

The atomic density in a dense, decaying, highly ionized hydrogen plasma has been measured directly. The measurements at 5 cm show that initially the degree of ionization is greater than 92%, the uncertainty in the atomic-density measurement being the source of uncertainty. It is probable that the degree of ionization is even higher.

At the inner radii the plasma is observed to recombine in place, its recombination rate being consistent with three-body recombination (see Appendix F).

An accounting of the plasma particles has been made. The reason the observed ion density is lower than the original filling is that considerable numbers of them are required for pressure balance at the ends of the plasma.

It has been determined that there is a layer of hydrogen atoms formed at the cylinder wall during the formation of the plasma. This layer is observed to move in radially in time.

Estimates of diffusion coefficients using the measured densities indicate that some process, possibly radiation, is playing a role in the removal of energy from the plasma.

ACKNOWLEDGMENTS

I wish to thank Dr. Wulf B. Kunkel for his interest and supervision and Dr. C. M. Van Atta for his support of this research. I particularly wish to express my appreciation to Dr. William S. Cooper III. His advice and encouragement on many occasions played a significant role in the completion of this experiment.

This work was done under the auspices of the U. S. Atomic Energy Commission.

APPENDICES

A. Relation of Emission Coefficient to Absorption Coefficient

For isotropic radiation the differential equation describing the radiant energy in the frequency interval dν is

$$\frac{dU_\nu}{d\ell}\,d\nu = 4\pi\epsilon_\nu d\nu - k_\nu U_\nu d\nu, \tag{34}$$

where ϵ_ν is the emission coefficient and k_ν is the absorption coefficient. Assuming equilibrium, $dU_\nu/d\ell = 0$ and U_ν is a black-body function. The emission and absorption coefficients are related by

$$\frac{\epsilon_\nu}{k_\nu} = \frac{2h\nu^3}{c^2}\,\frac{1}{e^{h\nu/kT} - 1}. \quad \text{(Kirchoff's Law)} \tag{35}$$

The absorption coefficient k_ν is related to the atomic absorption coefficient per atom in the ground state by

$$k_\nu = N_1(1 - e^{-h\nu/kT})\kappa_\nu. \tag{36}$$

The factor $(1 - e^{-h\nu/kT})$ corrects for stimulated emission

$$U_\nu d\nu = \frac{8\pi h\nu^3}{c^2}\,N_1 e^{-h\nu/kT}\kappa_\nu d\nu. \tag{37}$$

The ground-state atomic density N_1 may now be related to the electron-ion-density product by Saha's equation

$$N_1 = \frac{N_i N_e}{S(T)} = \frac{N_i N_e h^3 \exp\left[(\chi - \Delta\chi)/kT\right]}{(2\pi m_e k)^{3/2} T^{3/2}} \tag{38}$$

and thefore the normalized continuum intensity is

$$W_c(T,\nu) = \frac{8\pi h^4 \nu^3}{c^2(2\pi m_e k)^{3/2}} \frac{\exp\left[-h\nu/kT\right] \exp\left[(X - \Delta X)/kT\right] \kappa_\nu}{T^{3/2}} \qquad (39)$$

where X is the ionization potential of the ground state (13.5 eV) and ΔX is the lowering of the ionization potential due to Debye shielding. The other symbols have their conventional meaning.

B. Correction of Electron-Temperature Measurements Near the Wall to Include H^- Continuum

Agreement among the different measurements of the electron temperature and density throughout most of the plasma is good for all times of interest (see Fig. 26).* Of interest is the region near the wall, where the agreement is definitely not good. Figure 27 is a plot of the electron temperature as a function of time for the 7-cm radius. As can be seen, there is serious disagreement. One possible explanation for the discrepancy is that there may be another source of continuum radiation contributing to the measured light. Two likely candidates are H^- continuum and H_2^+ continuum. They are represented by the equations

$$H + e \rightarrow H^- + h\nu \qquad (40a)$$

and

$$H + H^+ \rightarrow H_2^+ + h\nu. \qquad (40b)$$

Since the absorption measurements have determined the ground-state atomic density, it should be possible to correct the measurements to include these contributions. Equation (27) becomes

$$\bar{I}_{c_{5305}} = N_i N_e W_{5305} + N_0 N_e G_{5305} + N_0 N_i F_{5305}, \qquad (41)$$

where G_{5305} is the H^- emission coefficient per ground-state hydrogen atom per electron and F_{5305} is the H_2^+ emission coefficient per

*Taken from Ref. 2 with the author's permission.

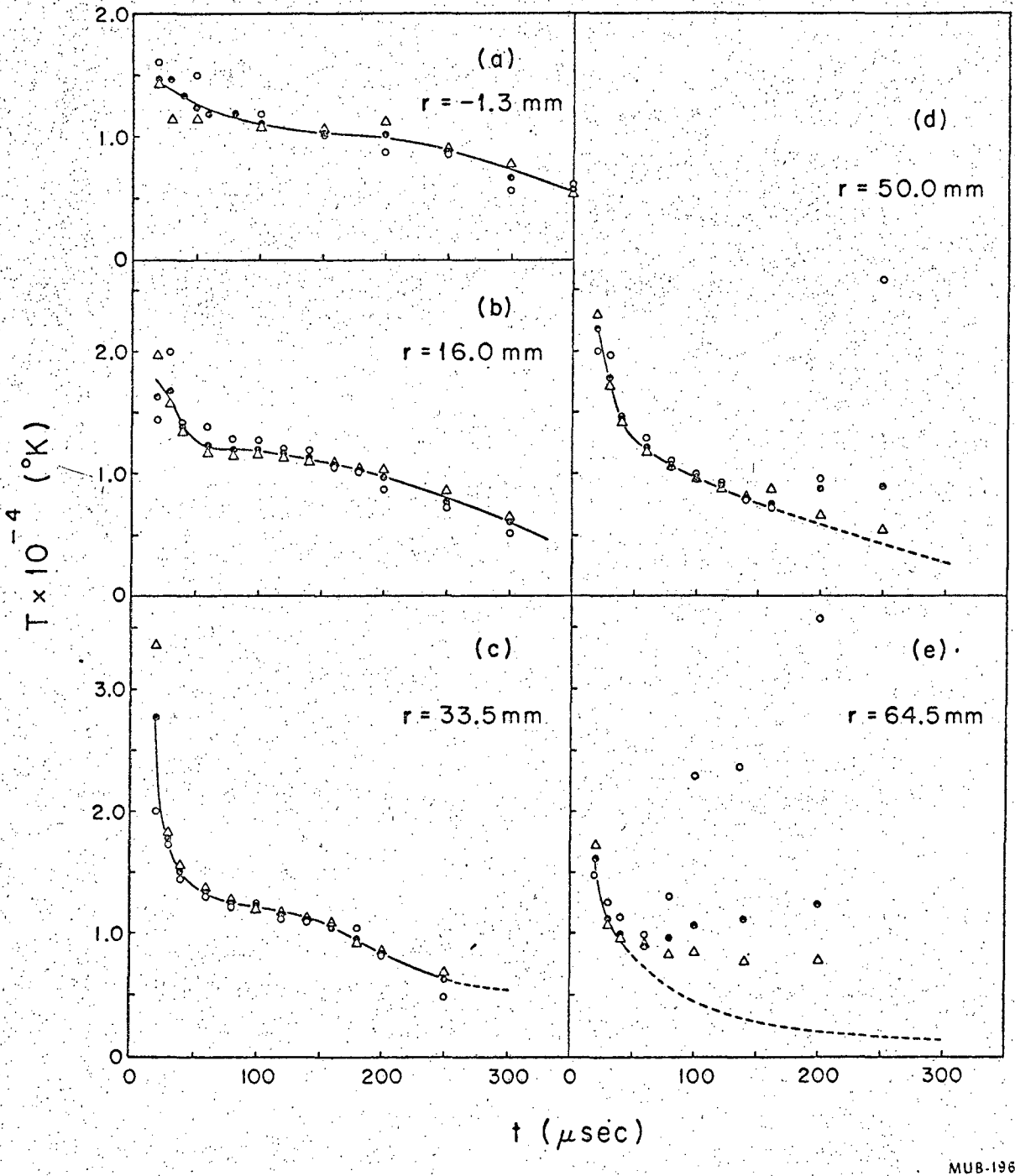

Fig. 26. Three temperature determinations from the three intensity measurements as a function of time five radii, looking parallel to the axis of the tube. Each point is an average of six shots. Solid dots, T(ℓ/v); triangles, T(ℓ/uv); and open dots, T(v/uv).

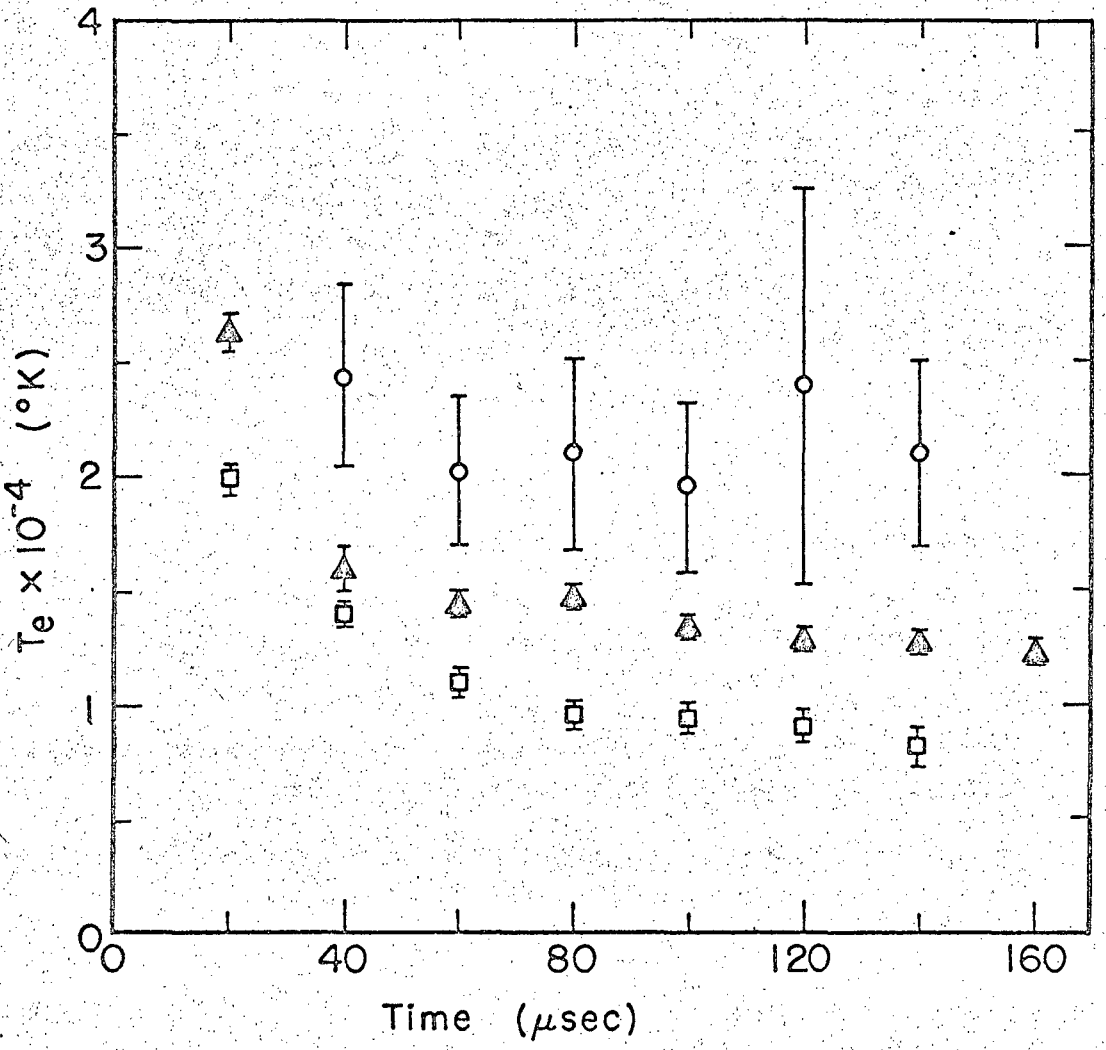

MUB-13837

Fig. 27. Three temperature determinations from the three intensity measurements at the 7-cm radius. Each point is the average of six shots. Squares, T(ℓ/uv); triangles, T(ℓ/v); and open dots, T(v/uv).

hydrogen atom per ion (see Fig. 28). Of the three measurements the 5305 Å is the only one affected significantly.

Figure 29 is the same data as Fig. 27 but includes this correction. There is a marked improvement.

Another possible source of error could arise if the H_β line were reabsorbed within the plasma. An estimate of this is possible from the calculations of Bates et al. The half width at half maximum of the hydrogen H_β spectral line due to Doppler broadening is

$$\Delta\lambda_D = 1.74\sqrt{T} \times 10^{-3}, \tag{42}$$

where T is expressed in °K and $\Delta\lambda$ in Å. From the calculations of Griem et al.,[34] the half width at half maximum due to Stark broadening is given by

$$\Delta\lambda_S = 7.3N_i^{2/3} \times 10^{-11} \tag{43a}$$

Therefore we have

$$\Delta\lambda_D/\Delta\lambda_S = 0.2384\sqrt{T}/N_i^{3/2}, \tag{43b}$$

where N_i is expressed in powers of 10^{15} and T in powers of 10^4. For conditions near the wall ($T = 7500°K$, $N = 10^{15}$), the Stark broadening is approximately six times the Doppler broadening.

One then asks, is H_β reabsorbed under these conditions of Stark broadening. To estimate this we introduce the spectral line profile P_ν with the normalization (P_ν is the probability of emission in ν to $\nu + d\nu$)

$$\int_0^\infty P_\nu(\nu)d\nu = 1. \tag{44}$$

The optical depth at the frequency ν is

$$\tau = 2.65 \times 10^{-2} f_{24} P_\nu N_2 L, \tag{45}$$

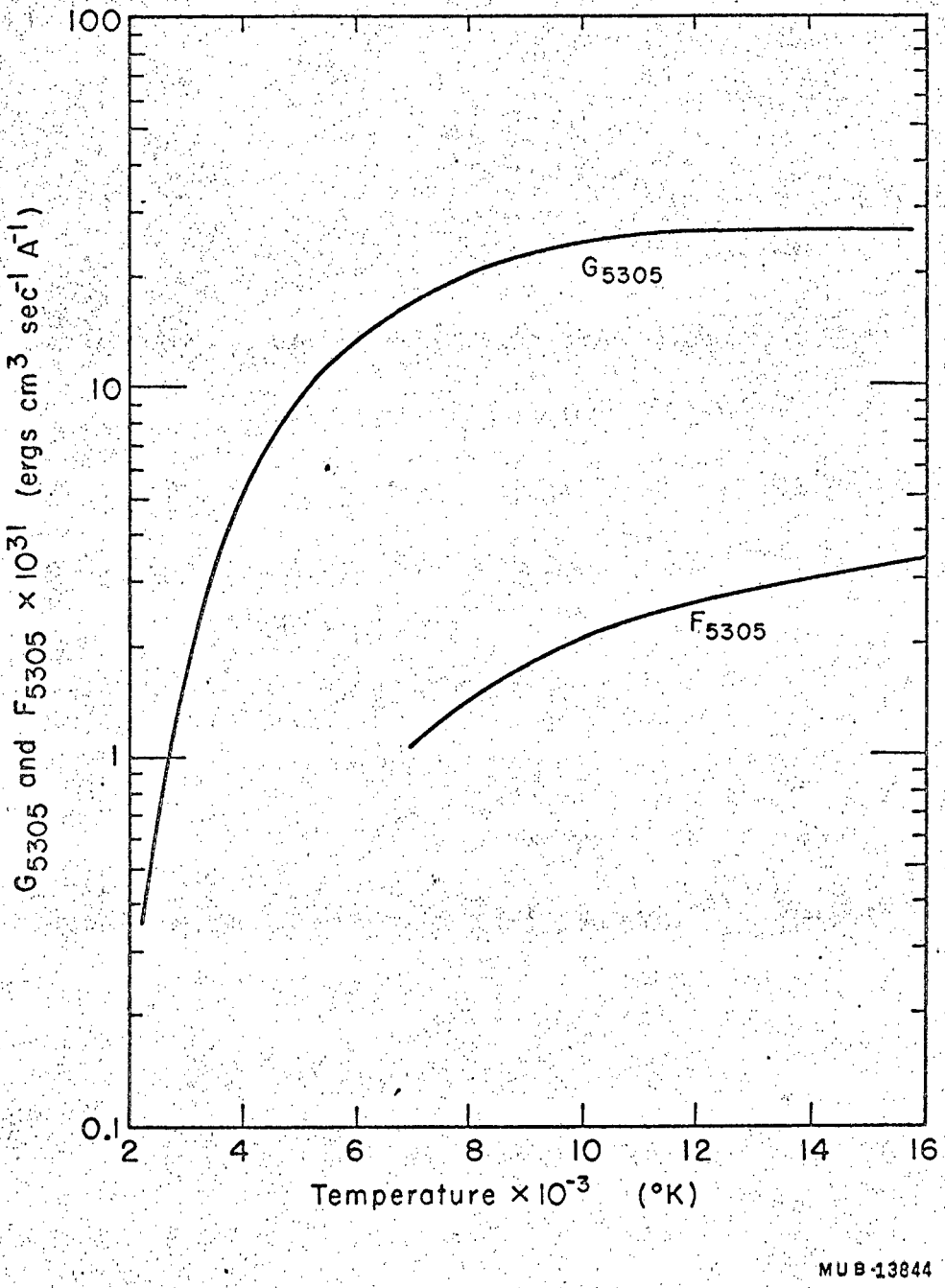

Fig. 28. Emission coefficients per hydrogen atom in the ground state per electron at a wavelength of 5305 Å. G_{5305} is the H^- coefficient and F_{5305} is that on H_2^+.

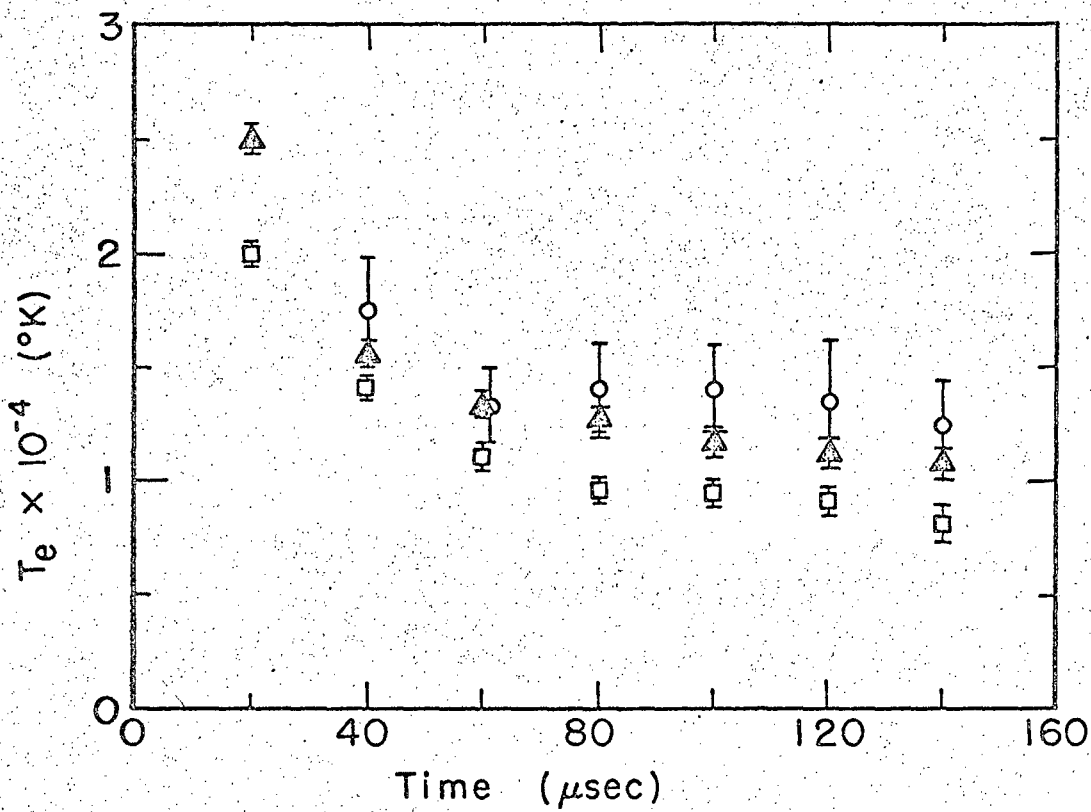

Fig. 29. Three temperature determinations from the three intensity measurements at the 7-cm radius, including the H^- and the H_2^+ correction using the measured atomic density.

where $f_{24} = 0.119$ is the H_β absorption oscillator strength, N_2 is the density of atoms in the lower state per cm^3, and L is the path length in cm. For the case of Stark broadening of hydrogen lines the spectral line profile may be expressed by

$$P_\nu = 10^8 \frac{\lambda_0^2}{c} \frac{S(\alpha)}{F_0}, \tag{46}$$

where F_0 is a normalized electric-field strength, $F_0 = eN_1^{2/3}$, e being the charge of the electron in esu, and $S(\alpha)$ are tabulated profiles most easily available in Ref. 34, pp. 445-452. Using a value of 5 for $S(\alpha)$ (an upper limit) and an electron density of 10^{15}, we have $P_\nu = 4.14 \times 10^{-12}$; therefore $\tau = 8.554 \times 10^{-13} N_2$ for L = 86.4 cm.

For the value of the number of atoms in the second level, the quasi-steady-state values for a decaying plasma that is opaque to Lyman lines of Bates et al. will be used. Assume

$$N_2 = 3.1 \times 10^{11}.$$

This yields an optical depth of 0.26. The light emitted from an optically thick medium is related to the emission of a similar optically thin medium by

$$I_{thick} = I_{thin} \left(\frac{1 - e^{-\tau}}{\tau} \right). \tag{47}$$

Therefore, in the case considered, approximately 90% of the light should be detected. This is not expected to introduce any significant error in the measured electron temperature, because the H_β light emitted is such a strong function of temperature (see Fig. 5).

The plasma emits far more light in the near uv at 3225 Å than it does at 5305 Å. This is the reason that the 5305-Å measurement was the only one affected by the H^- and the H_2^+ continuum. It would seem that the remaining discrepancy of the electron-temperature measurements

of Fig. 29 is possibly due to another "effective source of continuum" adding to the 5305-Å signal. This could be continuum due to impurities or possibly impurity lines. In either case the effect of such an extraneous signal would be to produce the observed errors. If the observed 5305-Å signals are first artificially reduced to 20 to 30%, and then the correction for the H^- and the H_2^+ is applied, excellent agreement is obtained. At later times in the discharge these corrections imply that less than 50% of the light detected is attributable to the radiative processes considered in the theory of Section IIC.

C. Absorption Measurements Very Late in Time

Absorption measurements very late in time were made at one radius (3 cm) for the full-length tube (Fig. 30). The plasma has never been studied for times greater than about 250 μsec. To decide whether volume recombination of the atoms is taking place or whether recombination is occurring primarily at the walls would require considerably more information about conditions present than is available. A good guess would be that the walls are playing a significant if not dominant role. It is satisfying, however, to observe the atoms recombining into molecules.

D. Representation of the Data

Figures 31 and 32 are plots of the atomic, ion, and total densities as a function of radius for several times. With such plots it is easy to visualize the decay of the atomic layer at the wall. No particular accuracy is claimed for the lines connecting the data points; however, the ion-density profile is known to have such a shape from previous measurements.[2] The atomic density must be a continuous function, and it seems reasonable to assume that it is monotonic. Therefore the profiles shown are probably not too far from the truth.

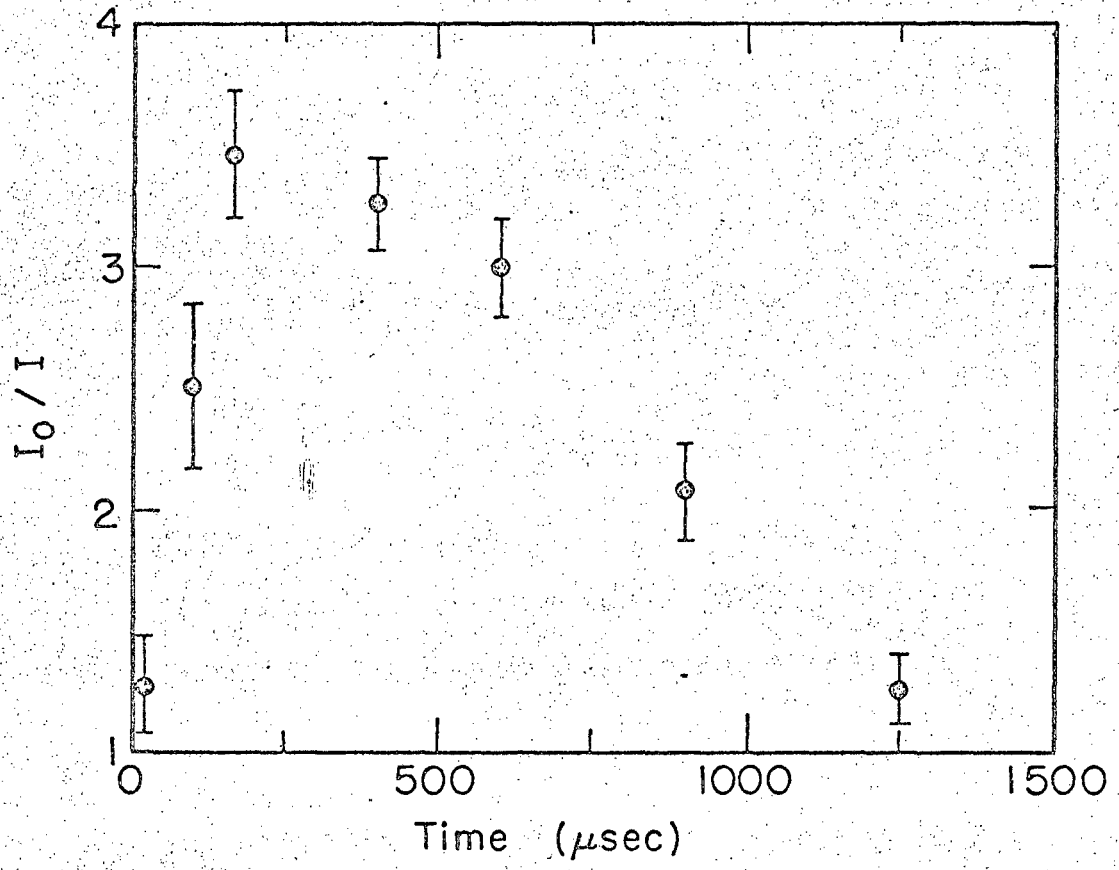

MUB-13836

Fig. 30. Absorption measurements late in time for the 3-cm radius. (L = 86.4 cm.)

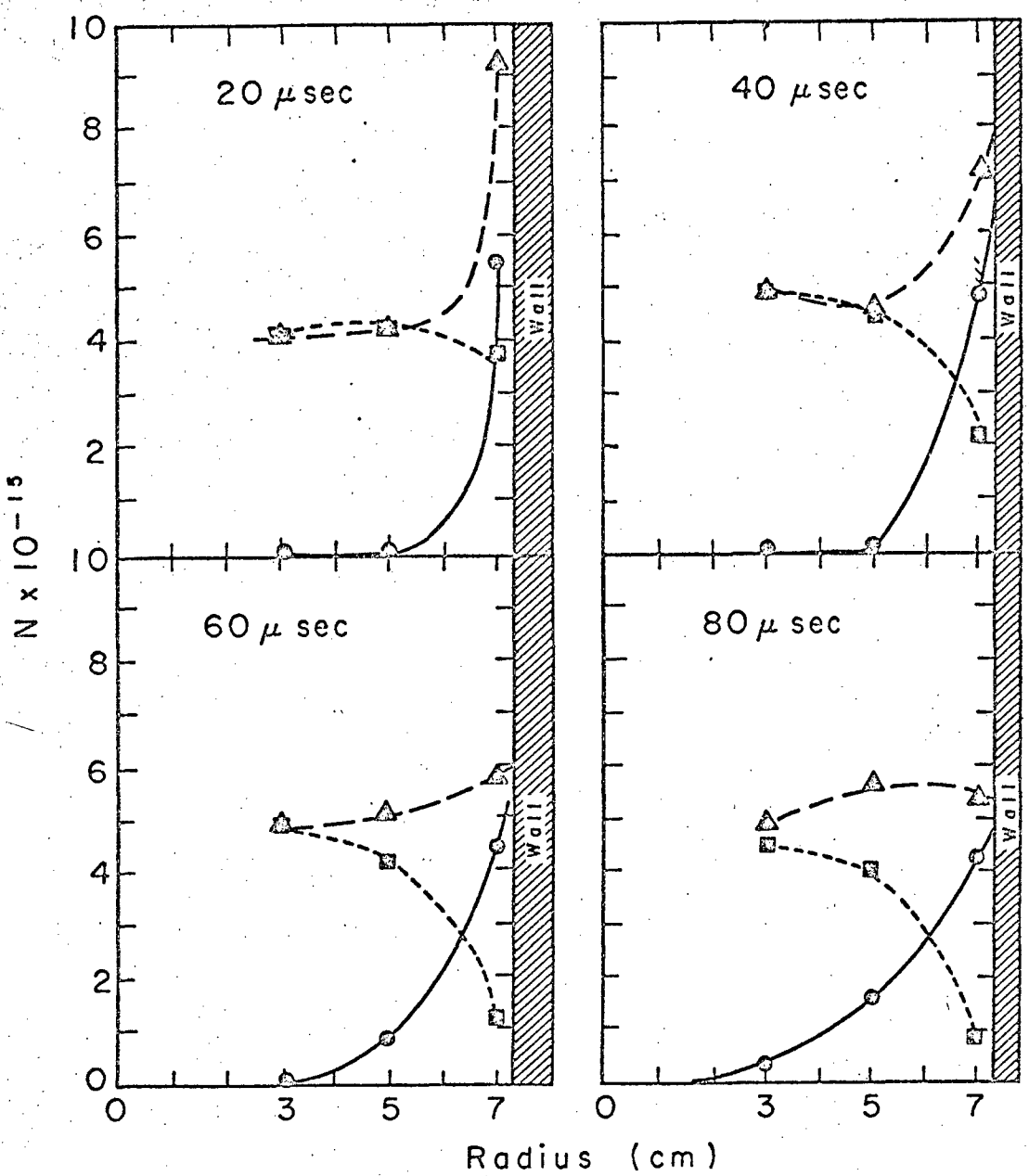

Fig. 31. Plots of the atomic, ion, and total density as a function of radius for several times. Dots indicate atomic density, squares indicate ion density.

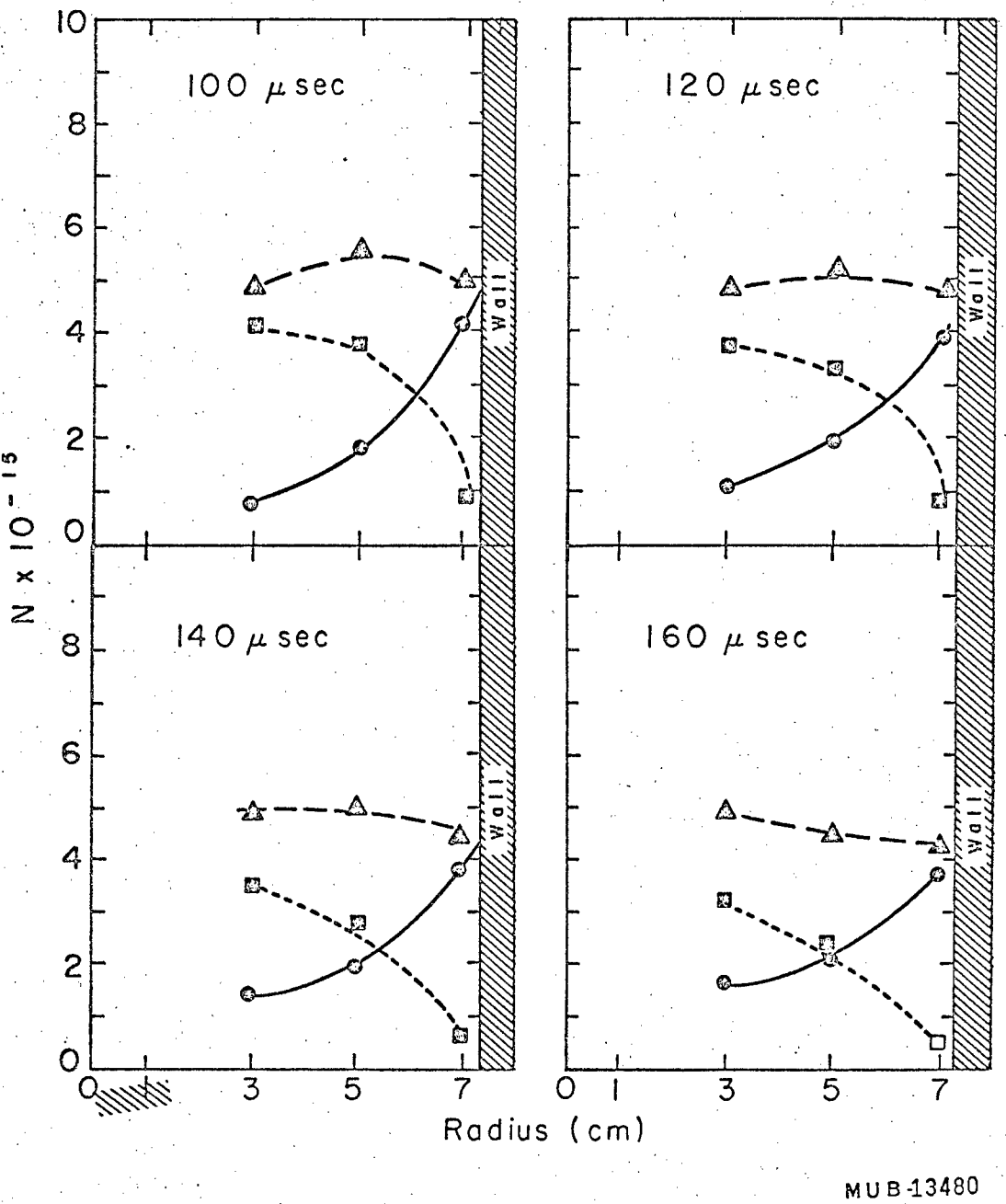

MUB-13480

Fig. 32. Plots of the atomic, ion, and total density as a function of radius for several times. Dots indicate atomic density, squares indicate ion density.

E. Comments on Lyman Alpha Radiation in This Plasma

To discuss the energy loss due to L_α radiation we much have some idea of the optical depth for the radiation. We will use Eq. (45) suitably modified:

$$\tau(\nu) = 2.65 \times 10^{-2} f_{12} P_\nu N_1 L. \tag{48}$$

For L_α the line profile is dominated by Doppler broadening. Therefore P_ν is

$$P_\nu = \frac{1}{\sqrt{\pi}} \frac{\lambda_0^2}{c} \frac{1}{W_D} \exp\left[-(\Delta\nu/W_D)^2\right], \tag{49}$$

where λ_0 is expressed in cm, and W_D is the half width at half maximum in cm; or

$$W_D = 3.56 \times 10^{-7} (\sqrt{T/m})\lambda_0, \tag{50}$$

where T is in ^oK and m is the mass in atomic units. For hydrogen at a temperature of 10^4 ^oK, this Doppler width is 4.33×10^{-10} cm. For a value of 10^{15} cm^{-3} for the ground-state density and an absorption oscillator strength of 0.4162, the optical depth is

$$\tau(\nu) = 140\ L \exp\left[-(\Delta\lambda/W_D)^2\right]. \tag{51}$$

The intensity at the center of the line falls to a value of 1/e in a distance of 7×10^{-3} cm. This distance is very much less than any macroscopic characteristic distance of the plasma. To get to a point where the optical depth is 1 cm, one must shift off the center of the line by over 3 times the half width at half maximum. The plasma therefore is truly optically thick for all but the very wings of the Doppler-broadened L_α line. The photons in the wings of the line will escape very rapidly. The line shape of the Lyman α line is expected to be distorted by this preferential loss. If there were some process that tried to repopulate the wings of the line at a sufficiently fast rate the energy loss in the line radiation would become significant.

The power readiated by optically thin plasmas as calculated by Bates et al.[26] is sufficient to explain the energy-loss rate observed in this plasma. However, this plasma is not optically thin to the lines of the Lyman series.

F. Observed Recombination-Rate Coefficient for the 3-cm Data

The recombination-rate coefficient as calculated from

$$\gamma(T,N) = \frac{\text{Observed rate of change of the electron density}}{(\text{Observed electron density})^2}$$

is plotted in Fig. 33. The squares are the experimental data, and the circles are values interpolated from the tables of Bates et al.[14] for plasmas optically thick to lines of the Lyman series. Considering that there may be uncertainties of factors of two or three in the cross sections employed by Bates et al. in their calculations, the very good agreement should probably be considered fortuitous.

The rate coefficient was calculated for times after 80 μsec. After this time the plasma is known to be rather uniform along its axis, making a comparison valid.[2,28]

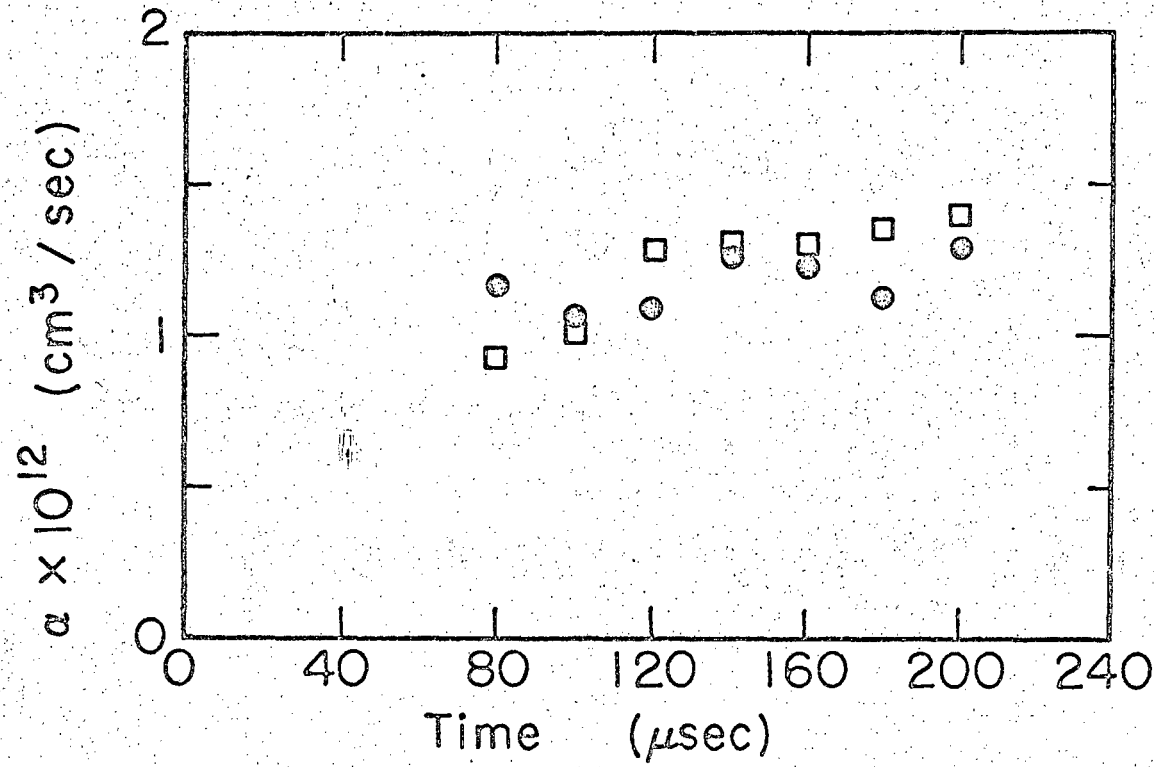

Fig. 33. Comparison of the observed decay coefficient with the calculations of Bates et al.[14] The solid dots are the experimental data.

REFERENCES

1. Lord Rayleigh, Long Duration of the Balmer Spectrum in Excited Hydrogen, Proc. Roy. Soc. (London) 183A, 26 (1944).
2. William S. Cooper III, An Experimental Investigation of the State of a Highly Ionized Decaying Hydrogen Plasma (Ph.D. Thesis), Lawrence Radiation Laboratory report UCRL-10849, June 17, 1963.
3. William S. Cooper III and Wulf B. Kunkel, Recombination of Ions and Electrons in a Highly Ionized Hydrogen Plasma, Phys. Rev. 138, 4A (1965).
4. E. Hinnov and J. G. Hirschberg, Spectroscopic Measurements of Helium Afterglow, in Ionization Phenomena in Gases (North-Holland Publishing Company, Amsterdam, 1962), Vol. 1, p. 638.
5. F. E. Irons and D. D. Millar, Measurements of the Decay Rate of a Hydrogen Plasma, J. Nucl. Energy: Pt. C, 7, 419 (1965).
6. F. Robben, Wulf B. Kunkel, and L. Talbot, Spectroscopic Study of Electron Recombination with Monatomic Ions in a Helium Plasma, Phys. Rev. 132, 2363 (1963).
7. J. D. Craggs and J. M. Meek, The Emission of Light from Spark Discharges, Proc. Roy. Soc. (London) 186A, 241 (1946).
8. H. Zanstra, Recombination and the Long Duration of the Balmer Spectrum, Proc. Roy. Soc. (London) 186A, 236 (1946).
9. N. D'Angelo, Recombination of Ions and Electrons, Phys. Rev. 121, 505 (1961).
10. E. Hinnov and J. G. Hirschberg, Electron-Ion Recombination in Dense Plasmas, Phys. Rev. 125, 795 (1962).
11. H. E. Stubbs, A. Dalgarno, D. Layser, E. N. Ashley, A. Naqvi, and G. Victor, Study of Recombination Phenomena, Vol. II Recombination in Plasma, Air Force Special Weapons Center Technical Documentary Report AFSWC-TDR-62-11 (1962) (unpublished).
12. M. J. Seaton, Radiative Recombination of Hydrogenic Ions, Monthly Notices Roy. Astron. Soc. 119, 81 (1959).
13. D. R. Bates, A. E. Kingston, and R. W. P. McWhirter, Recombination Between Electrons and Atomic Ions, I. Optically Thin Plasmas,